

Multivariate regression modeling in integrative analysis via sparse regularization

Shuichi Kawano¹, Toshikazu Fukushima²,
Junichi Nakagawa² and Mamoru Oshiki³

¹*Faculty of Mathematics, Kyushu University, 744 Motoooka Nishi-ku Fukuoka 819-0395,
Japan.*

skawano@math.kyushu-u.ac.jp

²*Advanced Technology Research Laboratories, Research & Development, Nippon Steel
Corporation, Futtsu, Chiba 293-8511, Japan.*

³*Division of Environmental Engineering, Faculty of Engineering, Hokkaido University,
Sapporo, Hokkaido 060-8628, Japan.*

Abstract

The multivariate regression model basically offers the analysis of a single dataset with multiple responses. However, such a single-dataset analysis often leads to unsatisfactory results. Integrative analysis is an effective method to pool useful information from multiple independent datasets and provides better performance than single-dataset analysis. In this study, we propose a multivariate regression modeling in integrative analysis. The integration is achieved by sparse estimation that performs variable and group selection. Based on the idea of alternating direction method of multipliers, we develop its computational algorithm that enjoys the convergence property. The performance of the proposed method is demonstrated through Monte Carlo simulation and analyzing wastewater treatment data with microbe measurements.

Key Words and Phrases: Group selection, Integrative analysis, Regularization, Sparsity, Wastewater treatment.

1 Introduction

Multivariate regression models are widely used for analyzing data with multiple continuous responses and have been studied exhaustively (Bedrick and Tsai, 1994; Liu et al., 1997; Rousseeuw et al., 2004; Peng et al., 2010; Obozinski et al., 2011; Qian et al., 2022). The

existing multivariate regression methods basically offer the analysis of a single dataset. However, single-dataset analysis causes models with low prediction accuracy and results with poor reproducibility (Tseng et al., 2015; Zhao et al., 2015). If there are multiple datasets from multiple independent studies with comparable designs, multi-datasets analysis can be used to extract useful information and increase sample size. Due to the property, multi-datasets analysis generally provides better performance than single-dataset analysis. Among multi-datasets analysis methods, integrative analysis has received considerable attention over the past decade (Zhao et al., 2015). A characteristic of integrative analysis is to analyze raw data from multiple datasets jointly and can outperform classical multi-datasets analysis methods such as meta-analysis, which pools summary statistic obtained by analyzing multiple datasets separately. Thus far, there have been many researches about integrative analysis: multiple regression (Liu et al., 2014; Huang et al., 2017b; Chang et al., 2022), logistic regression (Ma et al., 2011; Tang and Song, 2016), survival data analysis (Liu et al., 2011; Ma et al., 2012; Liu et al., 2013a,b; Cheng et al., 2015; Zhang et al., 2016; Deng et al., 2021; Tang and Song, 2021; Ventz et al., 2022), boosting (Huang et al., 2017a; Sun et al., 2020), and multivariate analysis (Fang et al., 2018; Dondelinger et al., 2020; Fan et al., 2020). Meanwhile, integrative analysis for multivariate regression models has not been fully explored.

In this article, we propose a multivariate regression modeling in integrative analysis. Multiple datasets are integrated by performing group selection across each dataset. The group selection is achieved by group lasso (Yuan and Lin, 2006). High-dimensional and low sample size data are becoming common in the current statistical context. To deal with such data, we perform model estimation and covariate selection simultaneously by lasso (Tibshirani, 1996). The computational algorithm of the proposed multivariate regression method is established by the technique of alternating direction method of multipliers (Boyd et al., 2011). We also show the convergence property of the algorithm.

The rest of this article is organized as follows. In Section 2, the proposed multivariate regression method is described. The computational algorithm and its theoretical property are described in Section 3. Simulation studies and analyzing wastewater treatment data

with microbiome measurement are contained in Section 4. Conclusions are given in Section 5.

2 Model

Let \mathbf{y} be a q -dimensional vector of response variables and \mathbf{x} be a p -dimensional vector of covariates. Suppose that we have M datasets for the variables: $\{(\mathbf{y}_i^m, \mathbf{x}_i^m); i = 1, \dots, n_m\}$ ($m = 1, \dots, M$), where n_m is a sample size of the m -th dataset. In addition, let \mathbf{z}^m be an r_m -dimensional vector of explanatory variables that are included in only the m -th dataset. For the variables, suppose that we obtain M datasets $\{\mathbf{z}_i^m; i = 1, \dots, n_m\}$ ($m = 1, \dots, M$).

We consider a multivariate regression model in the m -th dataset in the form

$$Y^m = \mathbf{1}_{n_m}(\boldsymbol{\alpha}^m)^\top + X^m B^m + Z^m C^m + E^m,$$

where $\mathbf{1}_{n_m}$ is an n_m -dimensional vector of which all components are one, $\boldsymbol{\alpha}^m$ is a q -dimensional vector of intercepts, $Y^m = (\mathbf{y}_1^m, \dots, \mathbf{y}_{n_m}^m)^\top$ is an $n_m \times q$ matrix of response variables, $X^m = (\mathbf{x}_1^m, \dots, \mathbf{x}_{n_m}^m)^\top$ is an $n_m \times p$ matrix of explanatory variables, B^m is a $p \times q$ matrix of coefficients, $Z^m = (\mathbf{z}_1^m, \dots, \mathbf{z}_{n_m}^m)^\top$ is an $n_m \times r_m$ matrix of explanatory variables included in only the m -th dataset, C^m is an $r_m \times q$ matrix of coefficients, and E^m is an $n_m \times q$ matrix of errors with mean $O_{n_m \times q}$ and variance-covariance matrix $I_{n_m} \otimes \Sigma$. Here, $O_{n_m \times q}$ is an $n_m \times q$ zero matrix, I_{n_m} is an $n_m \times n_m$ identity matrix, and Σ is a $q \times q$ positive definite matrix. We denote the (j, k) -th element of B^m as β_{jk}^m and set $\boldsymbol{\beta}_{jk} = (\beta_{jk}^1, \dots, \beta_{jk}^M)^\top$ ($j = 1, \dots, p; k = 1, \dots, q$). We assume homogeneity models: B^m 's have the same sparse structure across datasets such that $I(\beta_{jk}^1 = 0) = \dots = I(\beta_{jk}^M = 0)$ for all (j, k) .

To estimate the parameters $\boldsymbol{\alpha}^m, B^m, C^m$ under the homogeneity model, we consider the

following minimization problem

$$\min_{\substack{\boldsymbol{\alpha}^1, \dots, \boldsymbol{\alpha}^M \\ B^1, \dots, B^M \\ C^1, \dots, C^M}} \left[\sum_{m=1}^M \frac{1}{2n_m} \|Y^m - \mathbf{1}_{n_m}(\boldsymbol{\alpha}^m)^\top - X^m B^m - Z^m C^m\|_F^2 + \lambda \sum_{j=1}^p \sum_{k=1}^q \|\boldsymbol{\beta}_{jk}\|_2 + \gamma \sum_{m=1}^M \|C^m\|_1 \right], \quad (1)$$

where $\|\cdot\|_F$ is the Frobenous norm, λ and γ are regularization parameters with non-negative value, and $\|\cdot\|_q$ is the L_q ($q = 1, 2$) norm of a vector. The second term is the group lasso penalty, which guarantees the homogeneity structure of a model. The third term is the lasso penalty. This term induces variable selection for the variables \mathbf{z}^m ($m = 1, \dots, M$). In general, the group lasso includes the square of the number of dimensions of the parameter vector in the penalty term. Note that we omit it in this study, because it is the constant \sqrt{M} .

3 Computation

3.1 Estimation algorithm

We use the alternating direction method of multipliers (ADMM; Boyd et al. (2011)) to obtain an estimate of the parameters $\boldsymbol{\alpha}^1, \dots, \boldsymbol{\alpha}^M, B^1, \dots, B^M, C^1, \dots, C^M$. We first rewrite the minimization problem (1) as

$$\min_{\substack{\boldsymbol{\alpha}^1, \dots, \boldsymbol{\alpha}^M \\ B^1, \dots, B^M \\ C^1, \dots, C^M \\ D^1, \dots, D^M \\ \boldsymbol{\eta}_{11}, \dots, \boldsymbol{\eta}_{pq}}} \left[\sum_{m=1}^M \frac{1}{2n_m} \|Y^m - \mathbf{1}_{n_m}(\boldsymbol{\alpha}^m)^\top - X^m B^m - Z^m C^m\|_F^2 + \lambda \sum_{j=1}^p \sum_{k=1}^q \|\boldsymbol{\eta}_{jk}\|_2 + \gamma \sum_{m=1}^M \|D^m\|_1 \right] \\ \text{subject to } \boldsymbol{\eta}_{jk} = \boldsymbol{\beta}_{jk}, \quad C^m = D^m. \quad (2)$$

From the problem (2), we can obtain the scaled augmented Lagrangian

$$\sum_{m=1}^M \frac{1}{2n_m} \|Y^m - \mathbf{1}_{n_m}(\boldsymbol{\alpha}^m)^\top - X^m B^m - Z^m C^m\|_F^2 + \lambda \sum_{j=1}^p \sum_{k=1}^q \|\boldsymbol{\eta}_{jk}\|_2 + \gamma \sum_{m=1}^M \|D^m\|_1 \\ + \frac{\rho}{2} \sum_{j=1}^p \sum_{k=1}^q \|\boldsymbol{\eta}_{jk} - \boldsymbol{\beta}_{jk} + \mathbf{u}_{jk}\|_2^2 + \frac{\rho}{2} \sum_{m=1}^M \|C^m - D^m + V^m\|_F^2, \quad (3)$$

where \mathbf{u}_{jk} ($j = 1, \dots, p$; $k = 1, \dots, q$) and V^m ($m = 1, \dots, M$) are dual variables and ρ is a penalty parameter with a positive value.

When we set $(\boldsymbol{\alpha}^m)^\ell, (B^m)^\ell, (C^m)^\ell, (D^m)^\ell, \boldsymbol{\eta}_{jk}^\ell, \mathbf{u}_{jk}^\ell, (V^m)^\ell$ ($m = 1, \dots, M, j = 1, \dots, p, k = 1, \dots, q$) as the estimates of $\boldsymbol{\alpha}^m, B^m, C^m, D^m, \boldsymbol{\eta}_{jk}, \mathbf{u}_{jk}, V^m$ in the ℓ -th iteration, respectively, the idea of ADMM algorithm induces the parameter update as follows:

$$\begin{aligned}
(\boldsymbol{\alpha}^m)^{\ell+1} &= \arg \min_{\boldsymbol{\alpha}^m} \|Y^m - \mathbf{1}_{n_m}(\boldsymbol{\alpha}^m)^\top - X^m(B^m)^\ell - Z^m(C^m)^\ell\|_F^2, \\
(B^m)^{\ell+1} &= \arg \min_{B^m} \left[\frac{1}{2n_m} \|Y^m - \mathbf{1}_{n_m}\{(\boldsymbol{\alpha}^m)^{\ell+1}\}^\top - X^m B^m - Z^m(C^m)^\ell\|_F^2 \right. \\
&\quad \left. + \frac{\rho}{2} \|B^m - (H^m)^\ell - (U^m)^\ell\|_F^2 \right], \\
(C^m)^{\ell+1} &= \arg \min_{C^m} \left[\frac{1}{2n_m} \|Y^m - \mathbf{1}_{n_m}\{(\boldsymbol{\alpha}^m)^{\ell+1}\}^\top - X^m(B^m)^{\ell+1} - Z^m(C^m)^\ell\|_F^2 \right. \\
&\quad \left. + \frac{\rho}{2} \|C^m - (D^m)^\ell + (V^m)^\ell\|_F^2 \right], \\
(D^m)^{\ell+1} &= \arg \min_{D^m} \left[\frac{\rho}{2} \|(C^m)^{\ell+1} - D^m + (V^m)^\ell\|_F^2 + \gamma \|D^m\|_1 \right], \\
\boldsymbol{\eta}_{jk}^{\ell+1} &= \arg \min_{\boldsymbol{\eta}_{jk}} \left[\frac{\rho}{2} \|\boldsymbol{\eta}_{jk} - \boldsymbol{\beta}_{jk}^{\ell+1} + \mathbf{u}_{jk}^\ell\|_2^2 + \lambda \|\boldsymbol{\eta}_{jk}\|_2 \right], \\
\mathbf{u}_{jk}^{\ell+1} &= \mathbf{u}_{jk}^\ell + \boldsymbol{\eta}_{jk}^{\ell+1} - \boldsymbol{\beta}_{jk}^{\ell+1}, \\
(V^m)^{\ell+1} &= (V^m)^\ell + (C^m)^{\ell+1} - (D^m)^{\ell+1},
\end{aligned}$$

where H^m and U^m are, respectively, a matrix whose the (j, k) -th element is η_{jk}^m and u_{jk}^m . In the update of B^m , we note that the equation $\sum_{j=1}^p \sum_{k=1}^q \|\boldsymbol{\eta}_{jk} - \boldsymbol{\beta}_{jk} + \mathbf{u}_{jk}\|_2^2 = \sum_{m=1}^M \|B^m - H^m - U^m\|_F^2$ is used. The update formula of $\boldsymbol{\alpha}^m, B^m, C^m$ is easy to obtain. Meanwhile, minimization of D^m and $\boldsymbol{\eta}_{jk}$ can be done using soft-thresholding operator. We use two soft-thresholding operators: the soft-thresholding operator for a scalar and a vector, which is

$$S(a, b) = \text{sign}(a)(|a| - b)_+, \quad \mathcal{S}(\mathbf{c}, d) = \left(1 - \frac{d}{\|\mathbf{c}\|_2}\right)_+ \mathbf{c},$$

respectively. Here, a, b, d are scalars and \mathbf{c} is a vector. Overall, the update is summarized in Algorithm 1.

Algorithm 1 ADMM algorithm for multivariate regression model in integrative analysis

1. Initialization: $\ell = 0$ and $(\boldsymbol{\alpha}^m)^0, (B^m)^0, (C^m)^0, (D^m)^0, \boldsymbol{\eta}_{jk}^0, \mathbf{u}_{jk}^0, (V^m)^0$ ($m = 1, \dots, M, j = 1, \dots, p, k = 1, \dots, q$).

2. Update $\ell = \ell + 1$.

(a) $(\boldsymbol{\alpha}^m)^{\ell+1} = \frac{1}{n_m} \{Y^m - X^m(B^m)^\ell - Z^m(C^m)^\ell\}^\top \mathbf{1}_{n_m}$

(b) $(B^m)^{\ell+1} = \left\{ (X^m)^\top X^m + n_m \rho I_p \right\}^{-1} \left[(X^m)^\top [Y^m - \mathbf{1}_{n_m} \{(\boldsymbol{\alpha}^m)^{\ell+1}\}^\top - Z^m(C^m)^\ell] + n_m \rho \{ (H^m)^\ell + (U^m)^\ell \} \right]$

(c) $(C^m)^{\ell+1} = \left\{ (Z^m)^\top Z^m + n_m \rho I_{r_m} \right\}^{-1} \left[(Z^m)^\top \{Y^m - \mathbf{1}_{n_m} \{(\boldsymbol{\alpha}^m)^{\ell+1}\}^\top - X^m(B^m)^{\ell+1}\} + n_m \rho \{ (D^m)^\ell - (V^m)^\ell \} \right]$

(d) $((D^m)^{\ell+1})_{ij} = S \left(((C^m)^{\ell+1} + (V^m)^\ell)_{ij}, \frac{\gamma}{\rho} \right), \quad (i = 1, \dots, r_m; j = 1, \dots, q)$

(e) $\boldsymbol{\eta}_{jk}^{\ell+1} = \mathcal{S} \left(\boldsymbol{\beta}_{jk}^{\ell+1} - \mathbf{u}_{jk}^\ell, \frac{\lambda}{\rho} \right)$

(f) $\mathbf{u}_{jk}^{\ell+1} = \mathbf{u}_{jk}^\ell + \boldsymbol{\eta}_{jk}^{\ell+1} - \boldsymbol{\beta}_{jk}^{\ell+1}$

(g) $(V^m)^{\ell+1} = (V^m)^\ell + (C^m)^{\ell+1} - (D^m)^{\ell+1}$

3. Repeat Step 2 until convergence. In our numerical study, the convergence condition is that the ℓ_2 norm of the difference between two consecutive quantities of $\mathbf{z}(3)$ is smaller than a prefixed threshold.

We provide the property of Algorithm 1. We set $\boldsymbol{\theta} = ((\boldsymbol{\alpha}^1)^\top, \dots, (\boldsymbol{\alpha}^M)^\top, (\text{vec}(B^1))^\top, \dots, (\text{vec}(B^M))^\top, (\text{vec}(C^1))^\top, \dots, (\text{vec}(C^M))^\top)^\top$ and

$\mathcal{L}(\boldsymbol{\theta}) = \sum_{m=1}^M \|Y^m - \mathbf{1}_{n_m}(\boldsymbol{\alpha}^m)^\top - X^m B^m - Z^m C^m\|_F^2 / (2n_m) + \lambda \sum_{j=1}^p \sum_{k=1}^q \|\boldsymbol{\beta}_{jk}\|_2 + \gamma \sum_{m=1}^M \|C^m\|_1$. In addition, let $\boldsymbol{\theta}^\ell$ be the estimate of $\boldsymbol{\theta}$ in the ℓ -th iteration derived from

Algorithm 1. Then Algorithm 1 satisfies the following convergence property.

Theorem 1. *Assume that there exists at least one solution $\boldsymbol{\theta}^*$ of (1). Then $\lim_{\ell \rightarrow \infty} \mathcal{L}(\boldsymbol{\theta}^\ell) = \mathcal{L}(\boldsymbol{\theta}^*)$ holds. Furthermore, $\lim_{\ell \rightarrow \infty} \|\boldsymbol{\theta}^\ell - \boldsymbol{\theta}^*\|_2 = 0$ holds whenever $\boldsymbol{\theta}^*$ is a unique solution.*

Proof. See the supplementary material S1. □

In this theorem, we note that the L_2 norm in $\|\boldsymbol{\theta}^\ell - \boldsymbol{\theta}^*\|_2$ is not essential. This theorem also stands for general norms of a vector space.

3.2 Selection of tuning parameter

We have three tuning parameters: λ, γ, ρ . According to Boyd et al. (2011), the penalty parameter ρ is fixed as one. The two regularization parameters λ, γ are selected by K -fold cross-validation. When we divide the original m -th dataset into the K datasets $(Y_{(1)}^m, X_{(1)}^m, Z_{(1)}^m), \dots, (Y_{(K)}^m, X_{(K)}^m, Z_{(K)}^m)$, the objective function for the K -fold cross-validation is

$$\text{CV} = \frac{1}{K} \sum_{k=1}^K \sum_{m=1}^M \frac{1}{2n_m^{(k)}} \left\| Y_{(k)}^m - \mathbf{1}_{n_m^{(k)}} (\hat{\boldsymbol{\alpha}}_{(-k)}^m)^\top - X_{(k)}^m \hat{B}_{(-k)}^m - Z_{(k)}^m \hat{C}_{(-k)}^m \right\|_F^2, \quad (4)$$

where $\hat{\boldsymbol{\alpha}}_{(-k)}^m, \hat{B}_{(-k)}^m, \hat{C}_{(-k)}^m$ are the estimates of $\boldsymbol{\alpha}^m, B^m, C^m$, respectively, computed with the data excluding the k -th dataset, and $n_m^{(k)}$ means the sample size in m -th and k -th dataset.

We choose the values of the regularization parameters λ, γ from the minimizers of CV in (4).

4 Numerical study

4.1 Monte Carlo simulations

We investigated the usefulness of our proposed method through Monte Carlo simulations. Data were generated from the true model

$$Y^m = X^m B^* + Z^m C^{*m} + E^m, \quad (m = 1, \dots, M).$$

We considered $M = 2, 3$.

Regardless of the number of datasets, we set as follows. We set $q = 2$ and $B^* = (B_1^{*\top}, B_2^{*\top})^\top$. Here

$$B_1^* = \begin{pmatrix} 1 & 1 & 1 & 1 & 1 & 0 & 0 & 0 & 0 & 0 \\ 0 & 0 & 0 & 0 & 0 & 0.5 & 0.5 & 0.5 & 0.5 & 0.5 \end{pmatrix}^\top$$

and $B_2^* = O_{s \times 2}$. We considered $s = 5, 50$. Each row of the design matrix corresponding to B_1^* was independently generated from a multivariate normal distribution having mean zero vector and variance-covariance matrix of which the (i, j) -th element is $\rho_x^{|i-j|}$. We considered $\rho_x = 0.1, 0.9$. On the other hand, each element of the design matrix corresponding to B_2^* was independently generated from $N(0, 1)$. Each row of the error matrix E^m was independently generated from a multivariate normal distribution having mean zero vector and variance-covariance matrix of which the (i, j) -th element is $\rho_y^{|i-j|}$. We considered $\rho_y = 0.1, 0.9$. The sample size was set to $n = 15, 25, 50, 75$.

For the case $M = 2$, we set as follows. We set $C^{*m} = (C_1^{*m\top}, C_2^{*m\top})^\top$. Here

$$\begin{aligned} C_1^{*1} &= \begin{pmatrix} 1 & 1 & 1 & 1 & 1 & 0 & 0 & 0 & 0 & 0 \\ 0 & 0 & 0 & 0 & 0 & 0.5 & 0.5 & 0.5 & 0.5 & 0.5 \end{pmatrix}^\top, \\ C_1^{*2} &= \begin{pmatrix} 0 & 0 & 0 & 0 & 0 & 0.5 & 0.5 & 0.5 & 0.5 & 0.5 \\ 1 & 1 & 1 & 1 & 1 & 0 & 0 & 0 & 0 & 0 \end{pmatrix}^\top \end{aligned} \quad (5)$$

and $C_2^{*m} = O_{s \times 2}$. Each row of the design matrix for C_1^{*m} was generated from similar manner of that of B_1^* . Each element of the design matrix for C_2^{*m} was independently generated from $N(0, 1)$.

For the case $M = 3$, we set as follows. We set $C^{*m} = (C_1^{*m\top}, C_2^{*m\top}, C_3^{*m\top})^\top$. Here C_1^{*1} and C_1^{*2} were the same as in (5),

$$C_1^{*3} = \begin{pmatrix} 0 & 0 & 0 & 1 & 1 & 1 & 1 & 0.5 & 0.5 & 0.5 \\ 1 & 1 & 1 & 0.5 & 0.5 & 0.5 & 0.5 & 0 & 0 & 0 \end{pmatrix}^\top,$$

and $C_2^{*m} = O_{s \times 2}$. The generation of each row of the design matrix for C_1^{*m} and each element of the design matrix for C_2^{*m} was the same as in the case $M = 2$.

We compared our proposed multivariate regression method (MR) with univariate multiple regression method in integrative analysis (UR), multiple regression method estimated by lasso (lasso), multivariate regression method estimated by group lasso (mglasso), and multivariate regression method estimated by lasso (mlasso). For MR and UR, we used $K = 5$ in (4). The comparative methods lasso and mglasso were computed by the package **glmnet** in the software R.

The simulation was conducted 100 times. The performance was evaluated in terms of mean squared error (MSE) given by $\text{MSE} = E[(y - \hat{y})^2]$, false positive rate (FPR), and false negative rate (FNR). MSE was estimated by 1,000 random samples. FPR and FNR are defined as

$$\text{FPR} = \frac{1}{100} \sum_{k=1}^{100} \frac{|\{j : \hat{\zeta}_j^{(k)} \neq 0 \wedge \zeta_j^* = 0\}|}{|\{j : \zeta_j^* \neq 0\}|}, \quad \text{FNR} = \frac{1}{100} \sum_{k=1}^{100} \frac{|\{j : \hat{\zeta}_j^{(k)} = 0 \wedge \zeta_j^* \neq 0\}|}{|\{j : \zeta_j^* = 0\}|}.$$

Here, ζ_j^* is the true j -th element, $\hat{\zeta}_j^{(k)}$ is the estimated j -th element for the k -th simulation, and $|\{*\}|$ is the number of elements included in a set $\{*\}$, where we set $\zeta = (\text{vec}(B^1)^\top, \dots, \text{vec}(B^M)^\top, \text{vec}(C^1)^\top, \dots, \text{vec}(C^M)^\top)^\top$.

We summarize boxplots of MSE from Figures 1 to 4 for $M = 2$ and Figures S.1 to S.4 for $M = 3$ in the supplementary material S2. In the figures, D1 and D2 indicate, respectively, a first dataset and a second dataset, while R1 and R2 indicate, respectively, a first response variable and a second response variable. Therefore, the term ‘‘D1 & R1’’ means the result for a first response variable obtained by analyzing a first dataset. First, we discuss the results for $M = 2$. The lasso and mglasso provide relatively larger MSE than MR, UR, and mlasso. The mlasso gives the smallest MSE when n is small, while it is as small as or larger than MR and UR when n is large. The MR and UR produce similar MSE, but we note that the UR can sometimes have large variances (e.g., see Figures 1f and 1h). Next, we discuss those for $M = 3$. The overall result is the same as when $M = 2$. The mlasso in $M = 3$ is unstable, because it gives the smallest or largest MSE when $n = 15, 25$.

The results of FPR and FNR are summarized in Figures 5 to 8 for $M = 2$ and Figures S.5 to S.8 for $M = 3$. In the figures, for example, the term ‘‘FPR (D1)’’ represents the result for FPR obtained by analyzing a first dataset. As the overall result for $M = 3$ is the same as when $M = 2$, we describe the results for $M = 2$. First, we discuss the results for FPR. In many cases, lasso gives the smallest MSE when $n = 15, 25$, while lasso and mlasso are smallest when $n = 50, 75$. The MR and UR are larger than other methods when n is small, but they are as small as lasso and mlasso when n is large. The mlasso provides large variances when $n = 15, 25$. Next, we discuss for FNR. The MR and UR often give the smallest FNR, followed by mlasso. The lasso and mglasso have relatively large FNR.

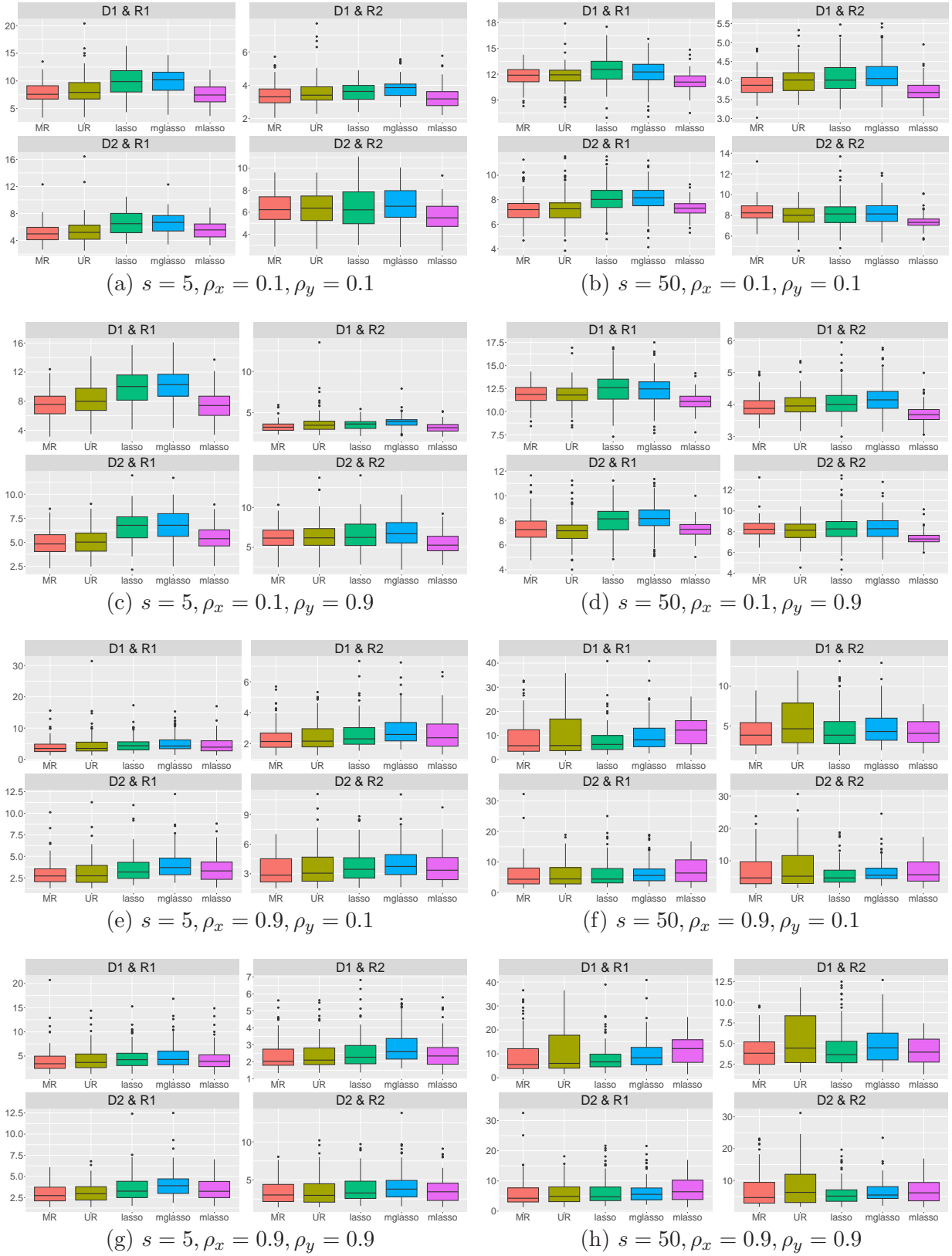


Figure 1: Boxplots of MSE for $n = 15$ when the case $M = 2$.

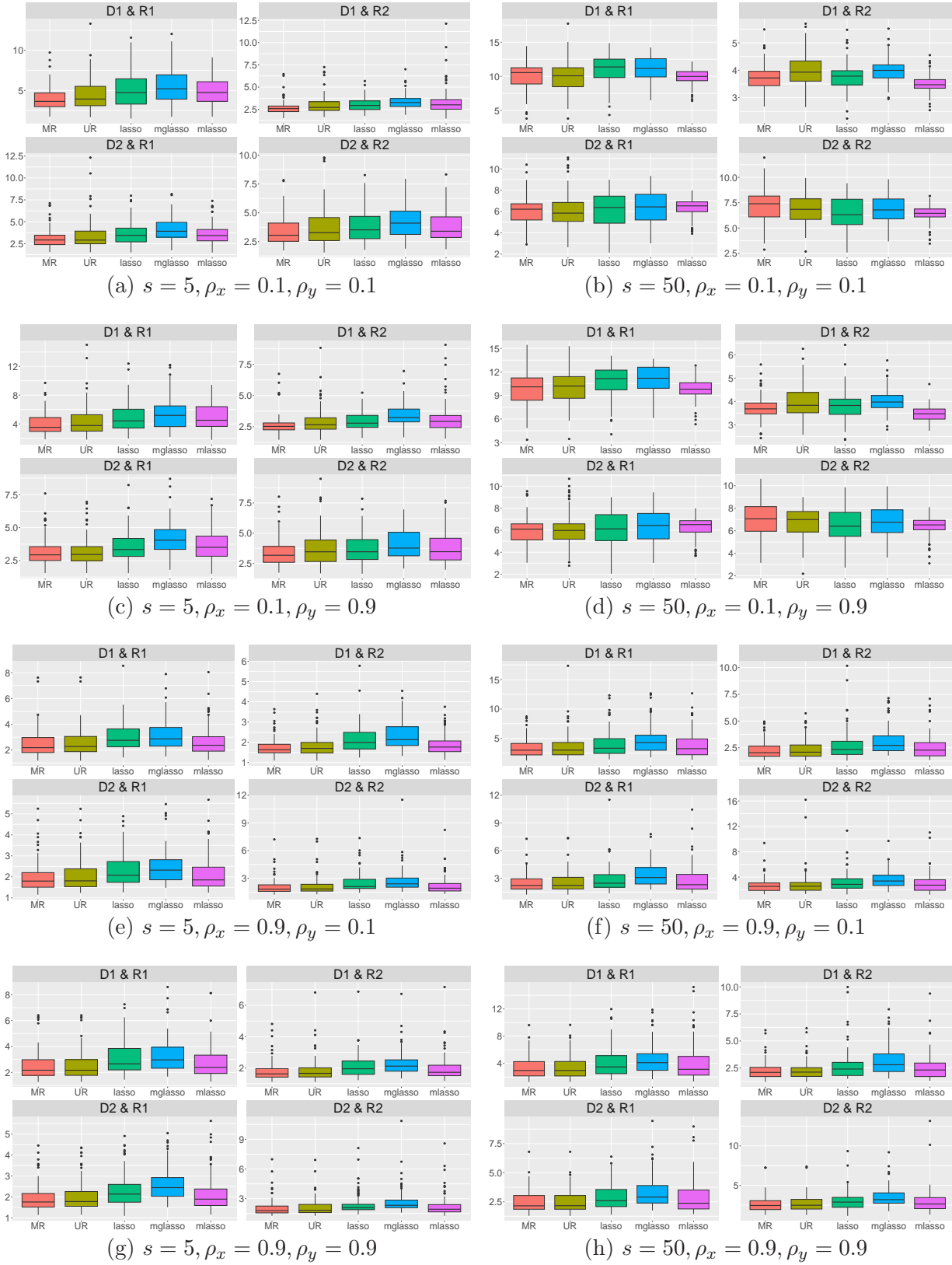


Figure 2: Boxplots of MSE for $n = 25$ when the case $M = 2$.

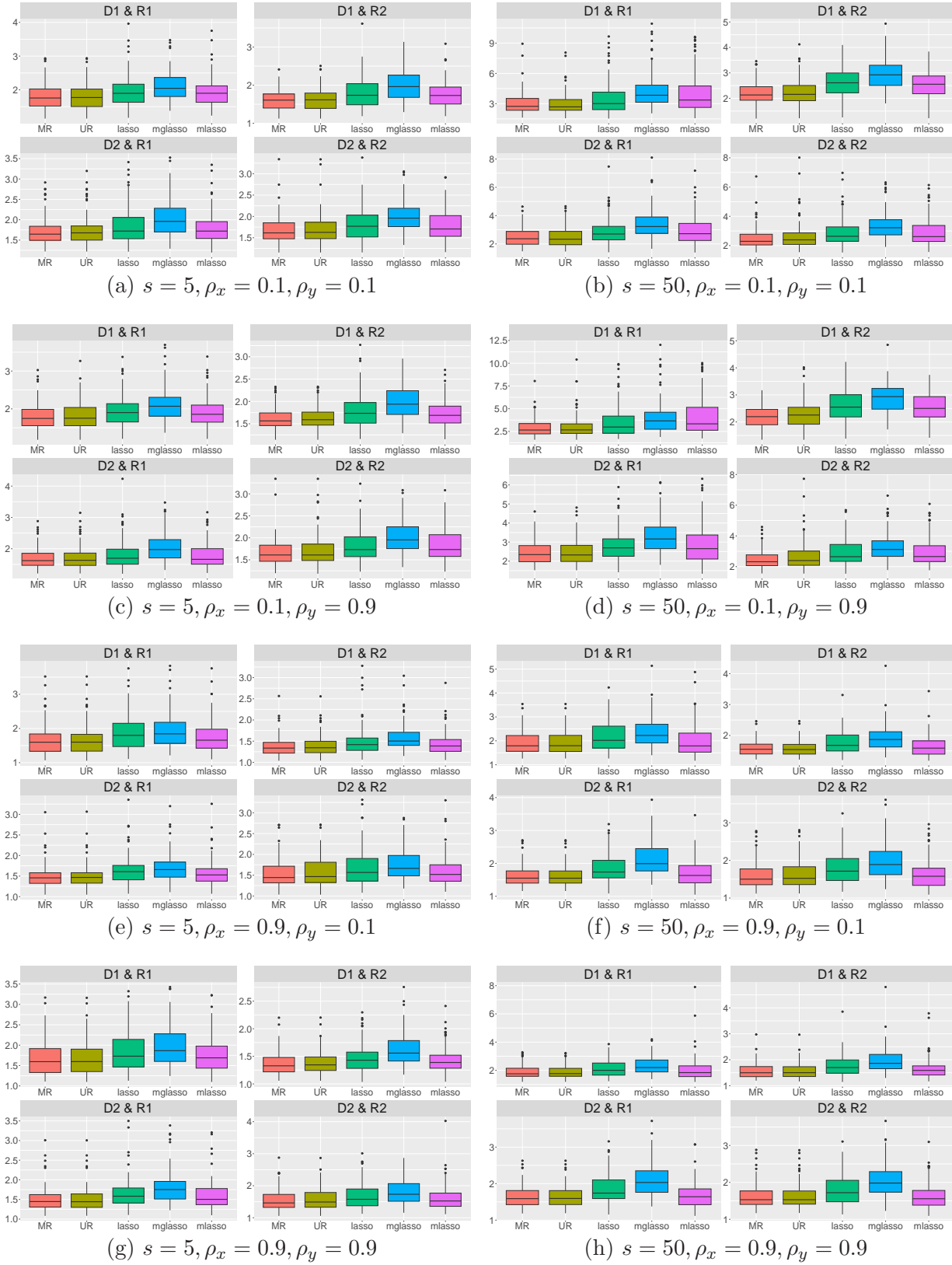


Figure 3: Boxplots of MSE for $n = 50$ when the case $M = 2$.

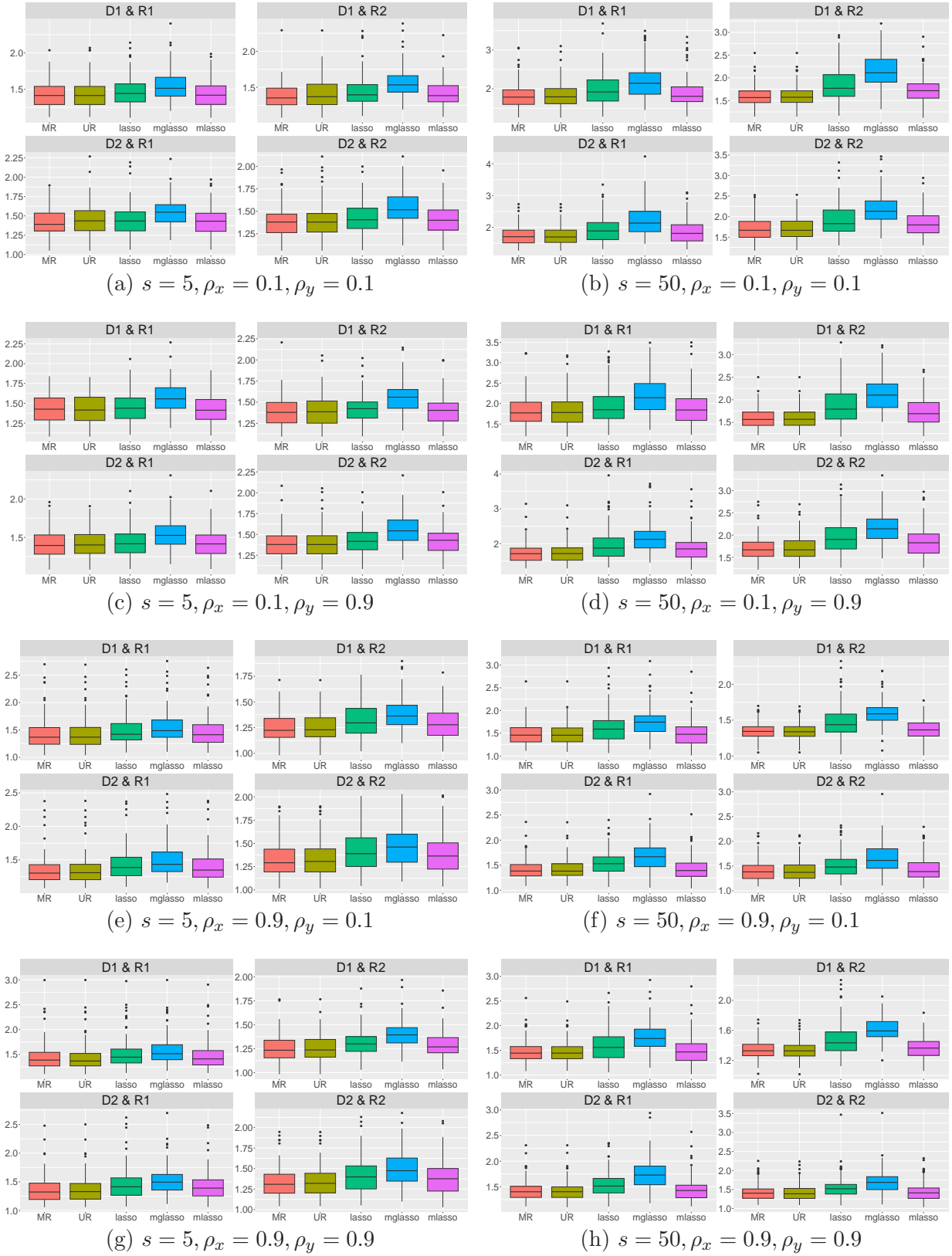


Figure 4: Boxplots of MSE for $n = 75$ when the case $M = 2$.



Figure 5: Boxplots of FPR and FNR for $n = 15$ when the case $M = 2$.

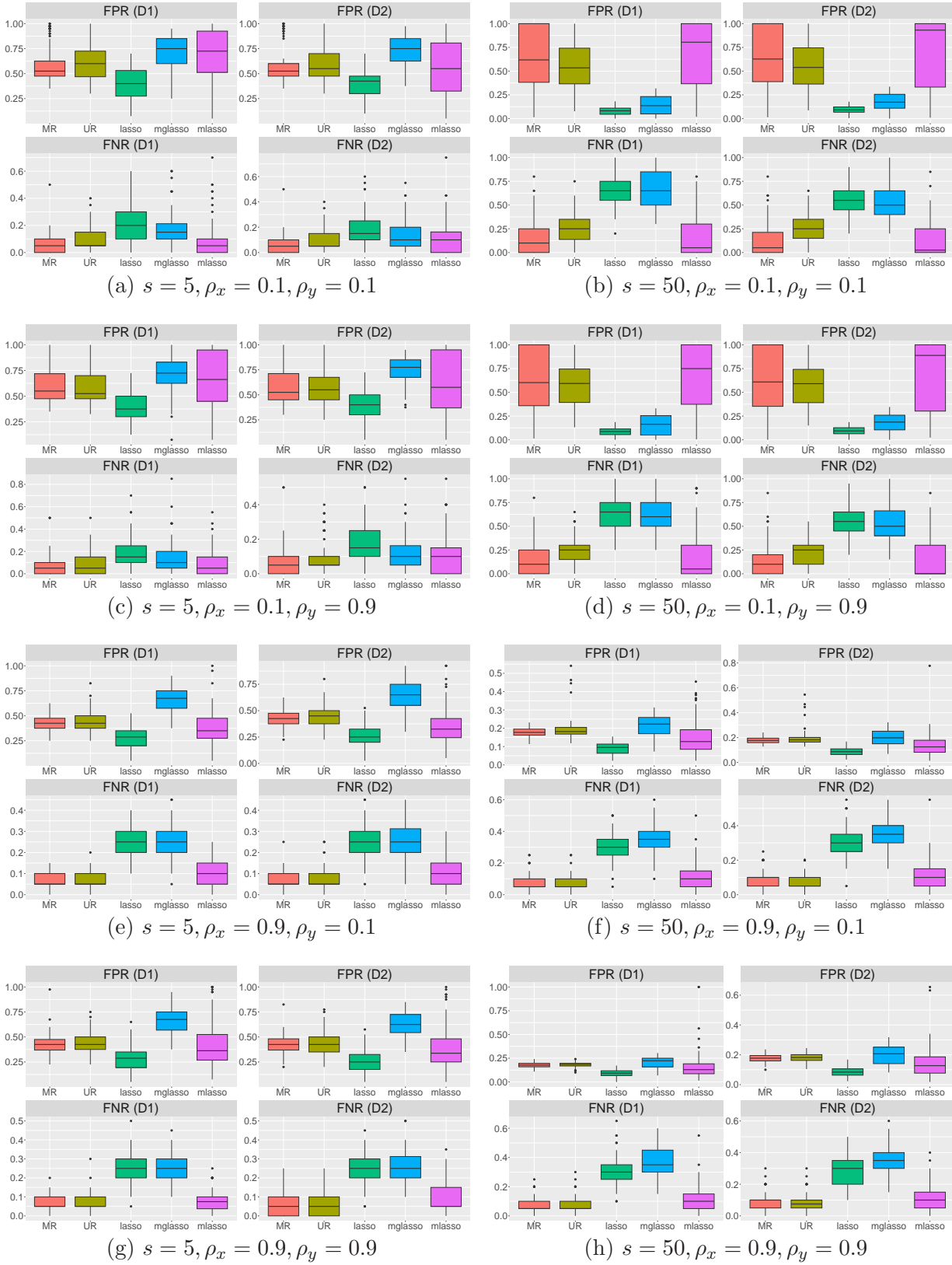


Figure 6: Boxplots of FPR and FNR for $n = 25$ when the case $M = 2$.



Figure 7: Boxplots of FPR and FNR for $n = 50$ when the case $M = 2$.

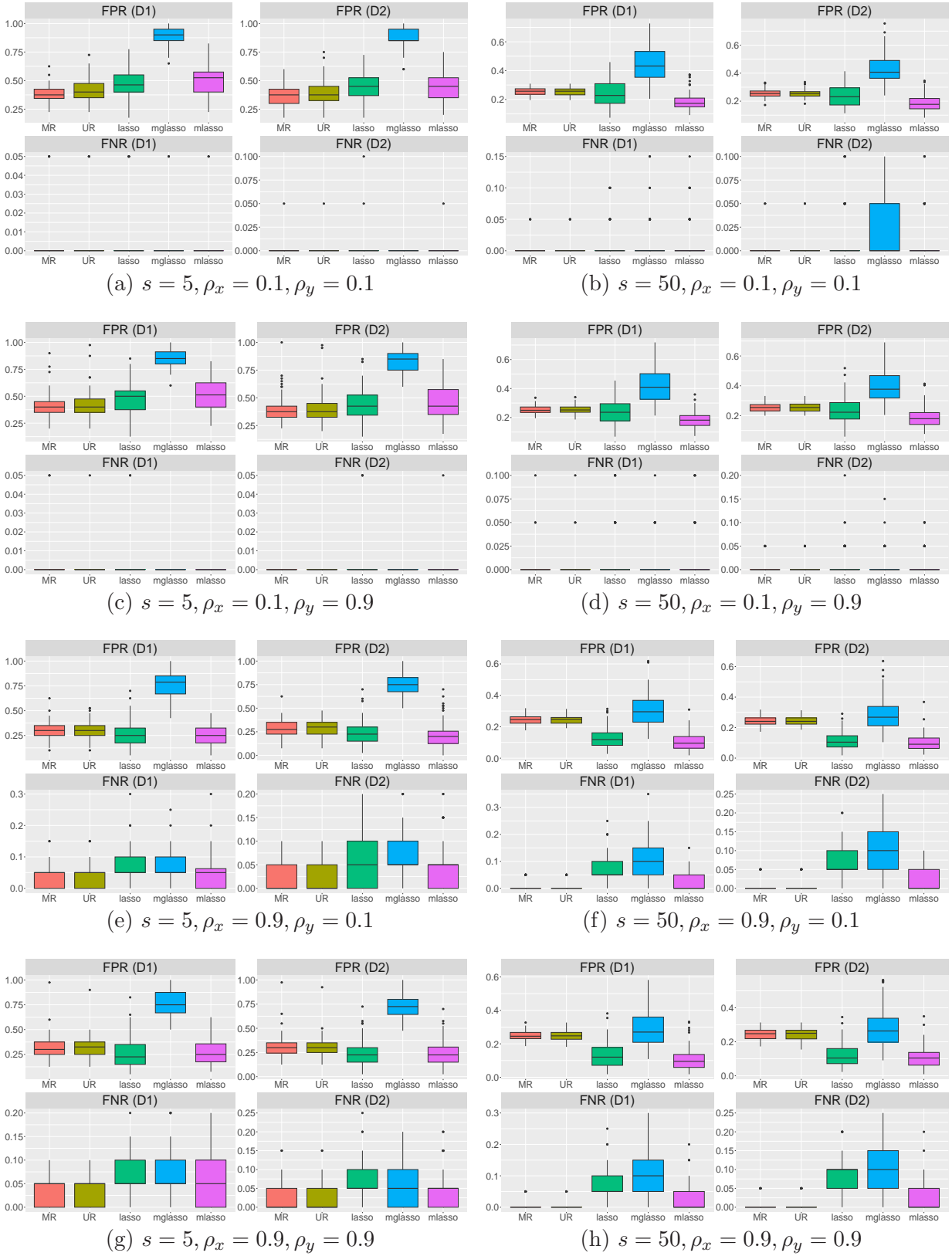


Figure 8: Boxplots of FPR and FNR for $n = 75$ when the case $M = 2$.

Table 1: Sample size and the numbers of covariates and responses in the wastewater treatment data.

Dataset No.	Sample size	# of covariates	# of responses
1	22	3,752	2
2	28	3,305	2
3	22	3,752	4
4	27	7,646	4

4.2 Application

We applied our proposed method into wastewater treatment data with microbe measurements. The data were obtained to find out the relationship between treatment of synthetic industrial wastewater and microbial species in the wastewater treatment (Fukushima et al., 2022). As industrial wastewater treatment, the rate (mg/L/day) of nitrite production (NO_2^-), thiocyanate degradation (SCN^-), phenol degradation ($\text{C}_6\text{H}_6\text{O}$), and thiosulfate degradation ($\text{S}_2\text{O}_3^{2-}$) were observed. The microbe data were obtained based on 16S rRNA gene sequencing using next generation sequencer. In this experiment, four datasets were given, which is summarized in Table 1. Note that the covariates and responses are corresponding to microbial species and industrial wastewater treatment, respectively. The responses in the first and second datasets consist of NO_2^- and SCN^- , while those in the third and fourth datasets do of NO_2^- , SCN^- , $\text{C}_6\text{H}_6\text{O}$, and $\text{S}_2\text{O}_3^{2-}$. For more details of these datasets, we refer to Fukushima et al. (2022).

We standardized the covariates for each dataset. We compared our proposed method with four methods in Section 4.1. To perform MR and UR, the datasets were preprocessed as follows. For Datasets 1 and 2, we extracted 227 microbial species commonly included among these datasets, 161 and 152 microbial species only included in Datasets 1 and 2, respectively. For Datasets 3 and 4, we extracted 215 microbial species commonly included among these datasets, 173 and 286 microbial species only included in Datasets 3 and 4, respectively. The value of tuning parameters in MR, UR, mlasso was selected by five-fold cross-validation,

Table 2: Cross-validated R^2 values for the wastewater treatment data. The bold value corresponds to the largest R^2 for each case.

Dataset No.	Wastewater treatment	MR	UR	lasso	mglasso	mlasso
1	NO ₂ ⁻	0.753	0.645	0.501	0.199	0.788
	SCN ⁻	0.899	0.899	0.596	0.604	0.914
2	NO ₂ ⁻	0.225	0.512	0.545	0.374	0.545
	SCN ⁻	0.741	0.741	0.403	0.444	0.733
3	NO ₂ ⁻	0.792	0.576	0.285	0.339	0.674
	SCN ⁻	0.782	0.665	0.524	0.586	0.667
	C ₆ H ₆ O	0.792	0.741	0.489	0.607	0.681
	S ₂ O ₃ ²⁻	0.794	0.773	0.539	0.605	0.686
4	NO ₂ ⁻	0.574	0.508	0.191	0.035	0.342
	SCN ⁻	0.776	0.651	0.634	0.466	0.683
	C ₆ H ₆ O	0.240	0.449	-0.039	-0.014	0.235
	S ₂ O ₃ ²⁻	0.725	0.692	0.130	0.412	0.627

while its value of lasso and mglasso was done by leave-one-out cross-validation by **glmnet**.

We computed the leave-one-out cross-validated R^2 value for each method. Table 2 summarizes the R^2 values. The mglasso method does not provide the largest value of R^2 for all cases. Although the lasso method provides the largest value once, it sometimes gives the smallest one for other cases. The mlasso has better results in Dataset 1. The UR method does not perform well compared to Monte Carlo simulations in Section 4.1. In many cases, the MR method is better than existing methods.

5 Conclusion and Discussion

We have presented a novel integrative analysis method in the framework of multivariate regression models. The integration has been achieved by group regularization. We have introduced a computational algorithm to obtain estimates of the parameters via ADMM. We have also provided the convergence property of the algorithm. Simulation results have

showed that our proposed method is competitive or better than competing approaches. In the analysis of wastewater treatment datasets, we have found that our proposed method often offers larger R^2 values than existing methods.

We note that there are some limitations for our proposed method. The squared loss function in the first term in (1) is simply extended as follows:

$$\text{tr} \left[\left\{ Y^m - \mathbf{1}_{n_m}(\boldsymbol{\alpha}^m)^\top - X^m B^m - Z^m C^m \right\} \Sigma \left\{ (Y^m - \mathbf{1}_{n_m}(\boldsymbol{\alpha}^m)^\top - X^m B^m - Z^m C^m)^\top \right\} \right].$$

This loss function explicitly includes correlation among responses. Thus, using this loss function may be expected to improve accuracy. In this article, we assume the homogeneity model. Recently, the heterogeneity model, which is defined such that $I(\beta_{jk}^1 = 0) = \dots = I(\beta_{jk}^M = 0)$ under some (j, k) holds while does not hold under others, has been intensively studied in integrative analysis (Huang et al., 2017b; Deng et al., 2021; Chang et al., 2022). It is of interest that our proposed method is extended into heterogeneity models by using sparse group regularization (Huang et al., 2012; Simon et al., 2013). In Section 4.2, we do not interpret the estimated coefficients. At present, many coefficient values are estimated as nonzero. By using non-convex penalties, e.g., SCAD (Fan and Li, 2001) and MCP (Zhang, 2010), the number of coefficients that are estimated by nonzero needs to be reduced a bit more in order to be interpretable. We leave them as a future research.

Acknowledgements

S. K. was supported by JSPS KAKENHI Grant Number JP19K11854.

References

- Bedrick, E. J. and Tsai, C.-L. (1994). Model selection for multivariate regression in small samples. *Biometrics*, 50(1):226–231.
- Boyd, S., Parikh, N., Chu, E., Peleato, B., and Eckstein, J. (2011). Distributed optimization

- and statistical learning via the alternating direction method of multipliers. *Foundations and Trends® in Machine Learning*, 3(1):1–122.
- Chang, C., Dai, Z., Oh, J., and Long, Q. (2022). Integrative learning of structured high-dimensional data from multiple datasets. *Statistical Analysis and Data Mining (early view)*.
- Cheng, X., Lu, W., and Liu, M. (2015). Identification of homogeneous and heterogeneous variables in pooled cohort studies. *Biometrics*, 71(2):397–403.
- Deng, S., Chen, J., and Shi, H. (2021). Integrative analysis of multiple types of genomic data using an accelerated failure time frailty model. *Computational Statistics*, 36:1499–1532.
- Dondelinger, F., Mukherjee, S., and Initiative, A. D. N. (2020). The joint lasso: high-dimensional regression for group structured data. *Biostatistics*, 21(2):219–235.
- Fan, J. and Li, R. (2001). Variable selection via nonconcave penalized likelihood and its oracle properties. *Journal of the American statistical Association*, 96(456):1348–1360.
- Fan, X., Fang, K., Ma, S., and Zhang, Q. (2020). Integrating approximate single factor graphical models. *Statistics in Medicine*, 39(2):146–155.
- Fang, K., Fan, X., Zhang, Q., and Ma, S. (2018). Integrative sparse principal component analysis. *Journal of Multivariate Analysis*, 166:1–16.
- Fukushima, T., Nakagawa, J., Kawano, S., and Oshiki, M. (2022). Development of statistical method for identification of microorganisms responsible for wastewater treatment. Technical Report 127, Nippon Steel Technical Report.
- Huang, J., Breheny, P., and Ma, S. (2012). A selective review of group selection in high-dimensional models. *Statistical Science*, 27(4):481–499.
- Huang, Y., Liu, J., Yi, H., Shia, B.-C., and Ma, S. (2017a). Promoting similarity of model sparsity structures in integrative analysis of cancer genetic data. *Statistics in Medicine*, 36(3):509–559.

- Huang, Y., Zhang, Q., Zhang, S., Huang, J., and Ma, S. (2017b). Promoting similarity of sparsity structures in integrative analysis with penalization. *Journal of the American Statistical Association*, 112(517):342–350.
- Liu, F., Dunson, D., and Zou, F. (2011). High-dimensional variable selection in meta-analysis for censored data. *Biometrics*, 67(2):504–512.
- Liu, J., Huang, J., and Ma, S. (2013a). Incorporating network structure in integrative analysis of cancer prognosis data. *Genetic Epidemiology*, 37(2):173–183.
- Liu, J., Ma, S., and Huang, J. (2014). Integrative analysis of cancer diagnosis studies with composite penalization. *Scandinavian Journal of Statistics*, 41(1):87–103.
- Liu, J., Wu, S., and Zidek, J. V. (1997). On segmented multivariate regression. *Statistica Sinica*, 7(2):497–525.
- Liu, M., Lu, W., Krogh, V., Hallmans, G., Clendenen, T. V., and Zeleniuch-Jacquotte, A. (2013b). Estimation and selection of complex covariate effects in pooled nested case-control studies with heterogeneity. *Biostatistics*, 14(4):682–694.
- Ma, S., Huang, J., and Song, X. (2011). Integrative analysis and variable selection with multiple high-dimensional data sets. *Biostatistics*, 12(4):763–775.
- Ma, S., Zhang, Y., Huang, J., Huang, Y., Lan, Q., Rothman, N., and Zheng, T. (2012). Integrative analysis of cancer prognosis data with multiple subtypes using regularized gradient descent. *Genetic Epidemiology*, 36(8):829–838.
- Obozinski, G., Wainwright, M. J., and Jordan, M. I. (2011). Support union recovery in high-dimensional multivariate regression. *The Annals of Statistics*, 39(1):1–47.
- Peng, J., Zhu, J., Bergamaschi, A., Han, W., Noh, D.-Y., Pollack, J. R., and Wang, P. (2010). Regularized multivariate regression for identifying master predictors with application to integrative genomics study of breast cancer. *The Annals of Applied Statistics*, 4(1):53–77.

- Qian, J., Tanigawa, Y., Li, R., Tibshirani, R., Rivas, M. A., and Hastie, T. (2022). Large-scale multivariate sparse regression with applications to uk biobank. *The Annals of Applied Statistics*, 16(3):1891–1918.
- Rousseeuw, P. J., Van Aelst, S., Van Driessen, K., and Gulló, J. A. (2004). Robust multivariate regression. *Technometrics*, 46(3):293–305.
- Simon, N., Friedman, J., Hastie, T., and Tibshirani, R. (2013). A sparse-group lasso. *Journal of Computational and Graphical Statistics*, 22(2):231–245.
- Sun, Y., Sun, Z., Jiang, Y., Li, Y., and Ma, S. (2020). An integrative sparse boosting analysis of cancer genomic commonality and difference. *Statistical Methods in Medical Research*, 29(5):1325–1337.
- Tang, L. and Song, P. X. (2016). Fused lasso approach in regression coefficients clustering: learning parameter heterogeneity in data integration. *The Journal of Machine Learning Research*, 17(1):3915–3937.
- Tang, L. and Song, P. X.-K. (2021). Poststratification fusion learning in longitudinal data analysis. *Biometrics*, 77(3):914–928.
- Tibshirani, R. (1996). Regression shrinkage and selection via the lasso. *Journal of the Royal Statistical Society Series B*, 58(1):267–288.
- Tseng, G., Ghosh, D., and Zhou, X. J. (2015). *Integrating Omics Data*. Cambridge University Press.
- Ventz, S., Mazumder, R., and Trippa, L. (2022). Integration of survival data from multiple studies. *Biometrics*, 78(4):1365–1376.
- Ye, G.-B. and Xie, X. (2011). Split bregman method for large scale fused lasso. *Computational Statistics & Data Analysis*, 55(4):1552–1569.

- Yuan, M. and Lin, Y. (2006). Model selection and estimation in regression with grouped variables. *Journal of the Royal Statistical Society: Series B (Statistical Methodology)*, 68(1):49–67.
- Zhang, C.-H. (2010). Nearly unbiased variable selection under minimax concave penalty. *The Annals of Statistics*, 38(2):894–942.
- Zhang, Q., Zhang, S., Liu, J., Huang, J., and Ma, S. (2016). Penalized integrative analysis under the accelerated failure time model. *Statistica Sinica*, 26(2):493–508.
- Zhao, Q., Shi, X., Huang, J., Liu, J., Li, Y., and Ma, S. (2015). Integrative analysis of ‘-omics’ data using penalty functions. *Wiley Interdisciplinary Reviews: Computational Statistics*, 7(1):99–108.

Supplementary Material for “Multivariate regression modeling in integrative analysis via sparse regularization”

by Shuichi Kawano, Toshikazu Fukushima, Junichi Nakagawa, Mamoru Oshiki

S1 Proof of Theorem 1

Here we prove Theorem 1. This proof is basically according to Ye and Xie (2011). In this proof, without loss of generality, we set $\boldsymbol{\alpha}^m = \mathbf{0}$ for $m = 1, \dots, M$.

Let $\mathcal{B}, \mathcal{C}, \mathcal{A}$ be

$$\mathcal{B} = \begin{pmatrix} \boldsymbol{\beta}_{11} & \cdots & \boldsymbol{\beta}_{p1} \\ \vdots & \ddots & \vdots \\ \boldsymbol{\beta}_{1q} & \cdots & \boldsymbol{\beta}_{pq} \end{pmatrix}, \quad \mathcal{C} = (C^1, \dots, C^M), \quad \mathcal{A} = \begin{pmatrix} \text{vec}(\mathcal{B}) \\ \text{vec}(\mathcal{C}) \end{pmatrix},$$

respectively. In addition, we define $V(\mathcal{A}) = \sum_{m=1}^M \|Y^m - X^m B^m - Z^m C^m\|_F^2 / (2n_m)$. Then, the first order optimality condition of Algorithm 1 provides

$$\left\{ \begin{array}{l} \mathbf{h}_{jk}^{\ell+1} - \rho(\boldsymbol{\eta}_{jk}^{\ell} - \boldsymbol{\beta}_{jk}^{\ell+1} + \mathbf{u}_{jk}^{\ell}) = \mathbf{0}, \\ \lambda \mathbf{s}_{jk}^{\ell+1} + \rho(\boldsymbol{\eta}_{jk}^{\ell+1} - \boldsymbol{\beta}_{jk}^{\ell+1} + \mathbf{u}_{jk}^{\ell}) = \mathbf{0}, \\ \mathbf{u}_{jk}^{\ell+1} = \mathbf{u}_{jk}^{\ell} + \boldsymbol{\eta}_{jk}^{\ell+1} - \boldsymbol{\beta}_{jk}^{\ell+1}, \\ (\mathbf{f}_k^m)^{\ell+1} + \rho \{ (\mathbf{c}_k^m)^{\ell+1} - (\mathbf{d}_k^m)^{\ell} + (\mathbf{v}_k^m)^{\ell} \} = \mathbf{0}, \\ \gamma (\mathbf{t}_k^m)^{\ell+1} - \rho \{ (\mathbf{c}_k^m)^{\ell+1} - (\mathbf{d}_k^m)^{\ell+1} + (\mathbf{v}_k^m)^{\ell} \} = \mathbf{0}, \\ (\mathbf{v}_k^m)^{\ell+1} = (\mathbf{v}_k^m)^{\ell} + (\mathbf{c}_k^m)^{\ell+1} - (\mathbf{d}_k^m)^{\ell+1}, \end{array} \right. \quad (\text{S.1})$$

for $j = 1, \dots, p$, $k = 1, \dots, q$, and $m = 1, \dots, M$. Here, $\mathbf{h}_{jk}^{\ell+1} = \frac{\partial V(\mathcal{A})}{\partial \boldsymbol{\beta}_{jk}} \Big|_{\mathcal{A}=\mathcal{A}^{\ell+1}}$, $\mathbf{s}_{jk}^{\ell+1} \in \partial \|\boldsymbol{\eta}_{jk}^{\ell+1}\|_2$ satisfying $\|\mathbf{s}_{jk}^{\ell+1}\|_2 \leq 1$, $(\mathbf{f}_k^m)^{\ell+1} = \frac{\partial V(\mathcal{A})}{\partial \mathbf{c}_k^m} \Big|_{\mathcal{A}=\mathcal{A}^{\ell+1}}$, and $(\mathbf{t}_k^m)^{\ell+1} \in \partial \|(\mathbf{d}_k^m)^{\ell+1}\|_1$.

When we set $\mathcal{A}^* = (\text{vec}(\mathcal{B}^*)^\top, \text{vec}(\mathcal{C}^*)^\top)^\top$ as a solution of (1), there exist \mathbf{h}_{jk}^* , \mathbf{s}_{jk}^* , $(\mathbf{f}_k^m)^*$,

$(\mathbf{t}_k^m)^*$ such that

$$\begin{cases} \mathbf{h}_{jk}^* + \lambda \mathbf{s}_{jk}^* = \mathbf{0}, \\ (\mathbf{f}_k^m)^* + \gamma (\mathbf{t}_k^m)^* = \mathbf{0}, \end{cases} \quad (\text{S.2})$$

for $j = 1, \dots, p$, $k = 1, \dots, q$, and $m = 1, \dots, M$. Here, $\mathbf{h}_{jk}^* = \frac{\partial V(\mathcal{A})}{\partial \beta_{jk}} \Big|_{\mathcal{A}=\mathcal{A}^*}$, $\mathbf{s}_{jk}^* \in \partial \|\beta_{jk}^*\|_2$, $(\mathbf{f}_k^m)^* = \frac{\partial V(\mathcal{A})}{\partial \mathbf{c}_k^m} \Big|_{\mathcal{A}=\mathcal{A}^*}$, $(\mathbf{t}_k^m)^* \in \partial \|(\mathbf{c}_k^m)^*\|_1$. By introducing variables $\boldsymbol{\eta}_{jk}^* = \beta_{jk}^*$, $\mathbf{u}_{jk}^* = -\lambda \mathbf{s}_{jk}^*/\rho$, $(\mathbf{d}_k^m)^* = (\mathbf{c}_k^m)^*$, $(\mathbf{v}_k^m)^* = \gamma (\mathbf{t}_k^m)^*/\rho$, we can rewrite (S.2) into two optimality conditions

$$\begin{cases} \mathbf{h}_{jk}^* - \rho(\boldsymbol{\eta}_{jk}^* - \beta_{jk}^* + \mathbf{u}_{jk}^*) = \mathbf{0}, \\ \lambda \mathbf{s}_{jk}^* + \rho(\boldsymbol{\eta}_{jk}^* - \beta_{jk}^* + \mathbf{u}_{jk}^*) = \mathbf{0}, \\ \mathbf{u}_{jk}^* = \mathbf{u}_{jk}^* + \boldsymbol{\eta}_{jk}^* - \beta_{jk}^*, \end{cases} \quad (\text{S.3})$$

for $j = 1, \dots, p$, $k = 1, \dots, q$ and

$$\begin{cases} (\mathbf{f}_k^m)^* + \rho \{(\mathbf{c}_k^m)^* - (\mathbf{d}_k^m)^* + (\mathbf{v}_k^m)^*\} = \mathbf{0}, \\ \gamma (\mathbf{t}_k^m)^* - \rho \{(\mathbf{c}_k^m)^* - (\mathbf{d}_k^m)^* + (\mathbf{v}_k^m)^*\} = \mathbf{0}, \\ (\mathbf{v}_k^m)^* = (\mathbf{v}_k^m)^* + (\mathbf{c}_k^m)^* - (\mathbf{d}_k^m)^*, \end{cases} \quad (\text{S.4})$$

for $m = 1, \dots, M$, $k = 1, \dots, q$. From (S.1), (S.3), and (S.4), we can find that $\boldsymbol{\eta}_{jk}^*$, β_{jk}^* , \mathbf{u}_{jk}^* , $(\mathbf{d}_k^m)^*$, $(\mathbf{c}_k^m)^*$, $(\mathbf{v}_k^m)^*$ are a fixed point of Algorithm 1.

First, we discuss (S.4). In this paragraph, we omit the index k, m . We denote the errors by

$$\mathbf{c}_e^\ell = \mathbf{c}^\ell - \mathbf{c}^*, \quad \mathbf{d}_e^\ell = \mathbf{d}^\ell - \mathbf{d}^*, \quad \mathbf{v}_e^\ell = \mathbf{v}^\ell - \mathbf{v}^*.$$

By subtracting the fourth equation in (S.1) by the first equation in (S.4), we have

$$\mathbf{f}^{\ell+1} - \mathbf{f}^* + \rho(\mathbf{c}_e^{\ell+1} - \mathbf{d}_e^\ell + \mathbf{v}_e^\ell) = \mathbf{0}.$$

Taking the inner product for this equality and \mathbf{c}_e^ℓ , we get

$$(\mathbf{f}^{\ell+1} - \mathbf{f}^*)^\top (\mathbf{c}_e^{\ell+1} - \mathbf{c}^*) + \rho \|\mathbf{c}_e^{\ell+1}\|_2^2 - \rho (\mathbf{d}_e^\ell)^\top (\mathbf{c}_e^{\ell+1}) + \rho (\mathbf{v}_e^\ell)^\top \mathbf{c}_e^{\ell+1} = 0. \quad (\text{S.5})$$

Similarly, we obtain

$$\gamma (\mathbf{t}^{\ell+1} - \mathbf{t}^*)^\top (\mathbf{d}_e^{\ell+1} - \mathbf{d}^*) - \rho (\mathbf{c}_e^{\ell+1})^\top \mathbf{d}_e^{\ell+1} + \rho \|\mathbf{d}_e^\ell\|_2^2 - \rho (\mathbf{v}_e^\ell)^\top \mathbf{d}_e^{\ell+1} = 0. \quad (\text{S.6})$$

To add the equations (S.5) and (S.6) leads to

$$\begin{aligned}
& (\mathbf{f}^{\ell+1} - \mathbf{f}^*)^\top (\mathbf{c}^{\ell+1} - \mathbf{c}^*) + \gamma (\mathbf{t}^{\ell+1} - \mathbf{t}^*)^\top (\mathbf{d}^{\ell+1} - \mathbf{d}^*) \\
& + \rho \left\{ \|\mathbf{c}_e^{\ell+1}\|_2^2 + \|\mathbf{d}_e^{\ell+1}\|_2^2 - (\mathbf{d}_e^\ell + \mathbf{d}_e^{\ell+1})^\top \mathbf{c}_e^{\ell+1} + (\mathbf{v}_e^\ell)^\top (\mathbf{c}_e^{\ell+1} - \mathbf{d}_e^{\ell+1}) \right\} = 0.
\end{aligned} \tag{S.7}$$

By subtracting the sixth equation in (S.1) by the third equation in (S.4), we have $\mathbf{v}_e^{\ell+1} = \mathbf{v}_e^\ell + \mathbf{c}_e^{\ell+1} - \mathbf{d}_e^{\ell+1}$. Taking square of both sides of this equation leads to

$$(\mathbf{v}_e^\ell)^\top (\mathbf{c}_e^{\ell+1} - \mathbf{d}_e^{\ell+1}) = \frac{1}{2} (\|\mathbf{v}_e^{\ell+1}\|_2^2 - \|\mathbf{v}_e^\ell\|_2^2) - \frac{1}{2} \|\mathbf{c}_e^{\ell+1} - \mathbf{d}_e^{\ell+1}\|_2^2. \tag{S.8}$$

By substituting (S.8) for (S.7), we obtain

$$\begin{aligned}
& (\mathbf{f}^{\ell+1} - \mathbf{f}^*)^\top (\mathbf{c}^{\ell+1} - \mathbf{c}^*) + \gamma (\mathbf{t}^{\ell+1} - \mathbf{t}^*)^\top (\mathbf{d}^{\ell+1} - \mathbf{d}^*) \\
& + \rho \left\{ \|\mathbf{c}_e^{\ell+1}\|_2^2 + \|\mathbf{d}_e^{\ell+1}\|_2^2 - (\mathbf{d}_e^\ell + \mathbf{d}_e^{\ell+1})^\top \mathbf{c}_e^{\ell+1} \right. \\
& \left. + \frac{1}{2} (\|\mathbf{v}_e^{\ell+1}\|_2^2 - \|\mathbf{v}_e^\ell\|_2^2) - \frac{1}{2} \|\mathbf{c}_e^{\ell+1} - \mathbf{d}_e^{\ell+1}\|_2^2 \right\} = 0.
\end{aligned} \tag{S.9}$$

Because the equation

$$\|\mathbf{x}\|_2^2 \pm \mathbf{x}^\top (\mathbf{y} + \mathbf{z}) + \|\mathbf{z}\|_2^2 = \frac{1}{2} \|\mathbf{x} \pm \mathbf{y}\|_2^2 + \frac{1}{2} \|\mathbf{x} \pm \mathbf{z}\|_2^2 + \frac{1}{2} (\|\mathbf{y}\|_2^2 - \|\mathbf{z}\|_2^2)$$

does hold for any $\mathbf{x}, \mathbf{y}, \mathbf{z} \in \mathbb{R}^p$, we obtain the following equation from the above equation and (S.9):

$$\begin{aligned}
& \frac{\rho}{2} (\|\mathbf{v}_e^\ell\|_2^2 - \|\mathbf{v}_e^{\ell+1}\|_2^2) + \frac{\rho}{2} (\|\mathbf{d}_e^\ell\|_2^2 - \|\mathbf{d}_e^{\ell+1}\|_2^2) \\
& = (\mathbf{f}^{\ell+1} - \mathbf{f}^*)^\top (\mathbf{c}^{\ell+1} - \mathbf{c}^*) + \gamma (\mathbf{t}^{\ell+1} - \mathbf{t}^*)^\top (\mathbf{d}^{\ell+1} - \mathbf{d}^*) + \frac{\rho}{2} \|\mathbf{c}_e^{\ell+1} - \mathbf{d}_e^\ell\|_2^2.
\end{aligned} \tag{S.10}$$

Since this equation holds for any m, k , we have

$$\begin{aligned}
& \frac{\rho}{2} \sum_{m,k} (\|(\mathbf{v}_k^m)_e\|_2^2 - \|(\mathbf{v}_k^m)_e^{\ell+1}\|_2^2) + \frac{\rho}{2} \sum_{m,k} (\|(\mathbf{d}_k^m)_e\|_2^2 - \|(\mathbf{d}_k^m)_e^{\ell+1}\|_2^2) \\
& = \sum_{m,k} \{(\mathbf{f}_k^m)^{\ell+1} - (\mathbf{f}_k^m)^*\}^\top \{(\mathbf{c}_k^m)^{\ell+1} - (\mathbf{c}_k^m)^*\} \\
& + \gamma \sum_{m,k} \{(\mathbf{t}_k^m)^{\ell+1} - (\mathbf{t}_k^m)^*\}^\top \{(\mathbf{d}_k^m)^{\ell+1} - (\mathbf{d}_k^m)^*\} + \frac{\rho}{2} \sum_{m,k} \|(\mathbf{c}_k^m)_e^{\ell+1} - (\mathbf{d}_k^m)_e^\ell\|_2^2.
\end{aligned} \tag{S.11}$$

By calculating for (S.3) in the same way, we can obtain

$$\begin{aligned}
& \frac{\rho}{2} \sum_{m,k} (\|(\mathbf{v}_k^m)_e\|_2^\ell - \|(\mathbf{v}_k^m)_e\|_2^{\ell+1}) + \frac{\rho}{2} \sum_{m,k} (\|(\mathbf{d}_k^m)_e\|_2^\ell - \|(\mathbf{d}_k^m)_e\|_2^{\ell+1}) \\
& + \frac{\rho}{2} \sum_{j,k} (\|(\mathbf{u}_{jk})_e\|_2^\ell - \|(\mathbf{u}_{jk})_e\|_2^{\ell+1}) + \frac{\rho}{2} \sum_{j,k} (\|(\boldsymbol{\eta}_{jk})_e\|_2^\ell - \|(\boldsymbol{\eta}_{jk})_e\|_2^{\ell+1}) \\
& = \sum_{m,k} \{(\mathbf{f}_k^m)^{\ell+1} - (\mathbf{f}_k^m)^*\}^\top \{(\mathbf{c}_k^m)^{\ell+1} - (\mathbf{c}_k^m)^*\} \\
& + \gamma \sum_{m,k} \{(\mathbf{t}_k^m)^{\ell+1} - (\mathbf{t}_k^m)^*\}^\top \{(\mathbf{d}_k^m)^{\ell+1} - (\mathbf{d}_k^m)^*\} + \frac{\rho}{2} \sum_{m,k} \|(\mathbf{c}_k^m)_e\|_2^{\ell+1} - (\mathbf{d}_k^m)_e\|_2^\ell \\
& + \sum_{j,k} (\mathbf{h}_{jk}^{\ell+1} - \mathbf{h}_{jk}^*)^\top (\boldsymbol{\beta}_{jk}^{\ell+1} - \boldsymbol{\beta}_{jk}^*) \\
& + \lambda \sum_{j,k} (\mathbf{s}_{jk}^{\ell+1} - \mathbf{s}_{jk}^*)^\top (\boldsymbol{\eta}_{jk}^{\ell+1} - \boldsymbol{\eta}_{jk}^*) + \frac{\rho}{2} \sum_{j,k} \|(\boldsymbol{\beta}_{jk})_e\|_2^{\ell+1} - (\boldsymbol{\eta}_{jk})_e\|_2^\ell.
\end{aligned}$$

Summing the above equation from $\ell = 0$ to $\ell = L$ brings in

$$\begin{aligned}
& \frac{\rho}{2} \sum_{m,k} (\|(\mathbf{v}_k^m)_e\|_2^0 - \|(\mathbf{v}_k^m)_e\|_2^{L+1}) + \frac{\rho}{2} \sum_{m,k} (\|(\mathbf{d}_k^m)_e\|_2^0 - \|(\mathbf{d}_k^m)_e\|_2^{L+1}) \\
& + \frac{\rho}{2} \sum_{j,k} (\|(\mathbf{u}_{jk})_e\|_2^0 - \|(\mathbf{u}_{jk})_e\|_2^{L+1}) + \frac{\rho}{2} \sum_{j,k} (\|(\boldsymbol{\eta}_{jk})_e\|_2^0 - \|(\boldsymbol{\eta}_{jk})_e\|_2^{L+1}) \\
& = \sum_{\ell=1}^L \sum_{m,k} \{(\mathbf{f}_k^m)^{\ell+1} - (\mathbf{f}_k^m)^*\}^\top \{(\mathbf{c}_k^m)^{\ell+1} - (\mathbf{c}_k^m)^*\} \\
& + \gamma \sum_{\ell=1}^L \sum_{m,k} \{(\mathbf{t}_k^m)^{\ell+1} - (\mathbf{t}_k^m)^*\}^\top \{(\mathbf{d}_k^m)^{\ell+1} - (\mathbf{d}_k^m)^*\} + \frac{\rho}{2} \sum_{\ell=1}^L \sum_{m,k} \|(\mathbf{c}_k^m)_e\|_2^{\ell+1} - (\mathbf{d}_k^m)_e\|_2^\ell \\
& + \sum_{\ell=1}^L \sum_{j,k} (\mathbf{h}_{jk}^{\ell+1} - \mathbf{h}_{jk}^*)^\top (\boldsymbol{\beta}_{jk}^{\ell+1} - \boldsymbol{\beta}_{jk}^*) \\
& + \lambda \sum_{\ell=1}^L \sum_{j,k} (\mathbf{s}_{jk}^{\ell+1} - \mathbf{s}_{jk}^*)^\top (\boldsymbol{\eta}_{jk}^{\ell+1} - \boldsymbol{\eta}_{jk}^*) + \frac{\rho}{2} \sum_{\ell=1}^L \sum_{j,k} \|(\boldsymbol{\beta}_{jk})_e\|_2^{\ell+1} - (\boldsymbol{\eta}_{jk})_e\|_2^\ell.
\end{aligned} \tag{S.12}$$

We note that the second and fifth terms in the right-hand side in (S.12) satisfy non-

negativity, because we have the following inequalities:

$$\begin{aligned}
(\mathbf{s}_{jk}^{\ell+1} - \mathbf{s}_{jk}^*)^\top (\boldsymbol{\eta}_{jk}^{\ell+1} - \boldsymbol{\eta}_{jk}^*) &= \|\boldsymbol{\eta}_{jk}^{\ell+1}\|_2^2 - \|\boldsymbol{\eta}_{jk}^*\|_2^2 - (\mathbf{s}_{jk}^*)^\top (\boldsymbol{\eta}_{jk}^{\ell+1} - \boldsymbol{\eta}_{jk}^*) \\
&\quad + \|\boldsymbol{\eta}_{jk}^*\|_2^2 - \|\boldsymbol{\eta}_{jk}^{\ell+1}\|_2^2 - (\mathbf{s}_{jk}^{\ell+1})^\top (\boldsymbol{\eta}_{jk}^* - \boldsymbol{\eta}_{jk}^{\ell+1}) \\
&\geq 0, \quad (\because \text{definition of sub-gradient.}) \\
\{(\mathbf{t}_k^m)^{\ell+1} - (\mathbf{t}_k^m)^*\}^\top \{(\mathbf{d}_k^m)^{\ell+1} - (\mathbf{d}_k^m)^*\} &= \|(\mathbf{d}_k^m)^{\ell+1}\|_1 - \|(\mathbf{d}_k^m)^*\|_1 \\
&\quad - \{(\mathbf{t}_k^m)^*\}^\top \{(\mathbf{d}_k^m)^{\ell+1} - (\mathbf{d}_k^m)^*\} \\
&\quad + \|(\mathbf{d}_k^m)^*\|_1 - \|(\mathbf{d}_k^m)^{\ell+1}\|_1 \\
&\quad - \{(\mathbf{t}_k^m)^{\ell+1}\}^\top \{(\mathbf{d}_k^m)^* - (\mathbf{d}_k^m)^{\ell+1}\} \\
&\geq 0. \quad (\because \text{definition of sub-gradient.})
\end{aligned}$$

In addition, when we set I^ℓ as a vector whose i -th element is defined by $\left. \frac{\partial V(\mathcal{A})}{\partial (\mathcal{A})_i} \right|_{\mathcal{A}=\mathcal{A}^\ell}$, the first and third terms also satisfy non-negativity from

$$\begin{aligned}
&\sum_{j,k} (\mathbf{h}_{jk}^{\ell+1} - \mathbf{h}_{jk}^*)^\top (\boldsymbol{\beta}_{jk}^{\ell+1} - \boldsymbol{\beta}_{jk}^*) + \sum_{m,k} \{(\mathbf{f}_k^m)^{\ell+1} - (\mathbf{f}_k^m)^*\}^\top \{(\mathbf{c}_k^m)^{\ell+1} - (\mathbf{c}_k^m)^*\} \\
&= -(I^*)^\top (\mathcal{A}^{\ell+1} - \mathcal{A}^*) + (I^{\ell+1})^\top (\mathcal{A}^{\ell+1} - \mathcal{A}^*) \\
&= V(\mathcal{A}^{\ell+1}) - V(\mathcal{A}^*) - (I^*)^\top (\mathcal{A}^{\ell+1} - \mathcal{A}^*) + V(\mathcal{A}^*) - V(\mathcal{A}^{\ell+1}) - (I^{\ell+1})^\top (\mathcal{A}^* - \mathcal{A}^{\ell+1}) \\
&\geq 0. \quad (\because \text{definition of gradient and convexity.})
\end{aligned} \tag{S.13}$$

These facts conclude that all terms in (S.12) are nonnegative. Thus, we have

$$\begin{aligned}
&\sum_{\ell=0}^{\infty} \left[\sum_{j,k} (\mathbf{h}_{jk}^{\ell+1} - \mathbf{h}_{jk}^*)^\top (\boldsymbol{\beta}_{jk}^{\ell+1} - \boldsymbol{\beta}_{jk}^*) + \sum_{m,k} \{(\mathbf{f}_k^m)^{\ell+1} - (\mathbf{f}_k^m)^*\}^\top \{(\mathbf{c}_k^m)^{\ell+1} - (\mathbf{c}_k^m)^*\} \right] \\
&\leq \frac{\rho}{2} \sum_{j,k} \|(\mathbf{u}_{jk})_e^0\|_2^2 + \frac{\rho}{2} \sum_{j,k} \|(\boldsymbol{\eta}_{jk})_e^0\|_2^2 + \frac{\rho}{2} \sum_{m,k} \|(\mathbf{v}_k^m)_e^0\|_2^2 + \frac{\rho}{2} \sum_{m,k} \|(\mathbf{d}_k^m)_e^0\|_2^2.
\end{aligned}$$

This leads to

$$\lim_{\ell \rightarrow \infty} \left[\sum_{j,k} (\mathbf{h}_{jk}^\ell - \mathbf{h}_{jk}^*)^\top (\boldsymbol{\beta}_{jk}^\ell - \boldsymbol{\beta}_{jk}^*) + \sum_{m,k} \{(\mathbf{f}_k^m)^\ell - (\mathbf{f}_k^m)^*\}^\top \{(\mathbf{c}_k^m)^\ell - (\mathbf{c}_k^m)^*\} \right] = 0.$$

From this convergence and (S.13), we can prove

$$\lim_{\ell \rightarrow \infty} [V(\mathcal{A}^\ell) - V(\mathcal{A}^*) - (I^*)^\top (\mathcal{A}^\ell - \mathcal{A}^*)] = 0. \tag{S.14}$$

Similarly, we have

$$\lim_{\ell \rightarrow \infty} \lambda \sum_{j,k} \{ \|\boldsymbol{\eta}_{jk}^\ell\|_2 - \|\boldsymbol{\eta}_{jk}^*\|_2 - (\mathbf{s}_{jk}^*)^\top (\boldsymbol{\eta}_{jk}^\ell - \boldsymbol{\eta}_{jk}^*) \} = 0,$$

$$\lim_{\ell \rightarrow \infty} \|\boldsymbol{\beta}_{jk}^\ell - \boldsymbol{\eta}_{jk}^\ell\|_2 = 0,$$

$$\lim_{\ell \rightarrow \infty} \gamma \sum_{m,k} [\|\mathbf{d}_k^m\|_1 - \|(\mathbf{d}_k^m)^*\|_1 - \{(\mathbf{t}_k^m)^*\}^\top \{(\mathbf{d}_k^m)^\ell - (\mathbf{d}_k^m)^*\}] = 0,$$

$$\lim_{\ell \rightarrow \infty} \|(\mathbf{c}_k^m)^\ell - (\mathbf{d}_k^m)^\ell\|_2 = 0.$$

Because the norms $\|\cdot\|_1, \|\cdot\|_2$ and the inner product are continuous and all norms on a finite dimensional space are equivalent, the equations

$$\lim_{\ell \rightarrow \infty} \lambda \sum_{j,k} \{ \|\boldsymbol{\beta}_{jk}^\ell\|_2 - \|\boldsymbol{\beta}_{jk}^*\|_2 - (\mathbf{s}_{jk}^*)^\top (\boldsymbol{\beta}_{jk}^\ell - \boldsymbol{\beta}_{jk}^*) \} = 0, \quad (\text{S.15})$$

$$\lim_{\ell \rightarrow \infty} \gamma \sum_{m,k} [\|\mathbf{c}_k^m\|_1 - \|(\mathbf{c}_k^m)^*\|_1 - \{(\mathbf{t}_k^m)^*\}^\top \{(\mathbf{c}_k^m)^\ell - (\mathbf{c}_k^m)^*\}] = 0 \quad (\text{S.16})$$

hold. From the equations (S.14), (S.15), (S.16), we obtain

$$\begin{aligned} & \lim_{\ell \rightarrow \infty} V(\mathcal{A}^\ell) - V(\mathcal{A}^*) - (I^*)^\top (\mathcal{A}^\ell - \mathcal{A}^*) \\ & + \lambda \sum_{j,k} \{ \|\boldsymbol{\beta}_{jk}^\ell\|_2 - \|\boldsymbol{\beta}_{jk}^*\|_2 - (\mathbf{s}_{jk}^*)^\top (\boldsymbol{\beta}_{jk}^\ell - \boldsymbol{\beta}_{jk}^*) \} \\ & + \gamma \sum_{m,k} [\|\mathbf{c}_k^m\|_1 - \|(\mathbf{c}_k^m)^*\|_1 - \{(\mathbf{t}_k^m)^*\}^\top \{(\mathbf{c}_k^m)^\ell - (\mathbf{c}_k^m)^*\}] = 0 \\ \Leftrightarrow & \lim_{\ell \rightarrow \infty} V(\mathcal{A}^\ell) + \lambda \sum_{j,k} \|\boldsymbol{\beta}_{jk}^\ell\|_2 + \gamma \sum_{m,k} \|(\mathbf{c}_k^m)^\ell\|_1 \\ & - \left\{ V(\mathcal{A}^*) + \lambda \sum_{j,k} \|\boldsymbol{\beta}_{jk}^*\|_2 + \gamma \sum_{m,k} \|(\mathbf{c}_k^m)^*\|_1 \right\} \\ & - \underbrace{\left[(I^*)^\top (\mathcal{A}^\ell - \mathcal{A}^*) + \lambda \sum_{j,k} (\mathbf{s}_{jk}^*)^\top (\boldsymbol{\beta}_{jk}^\ell - \boldsymbol{\beta}_{jk}^*) + \gamma \sum_{m,k} \{(\mathbf{t}_k^m)^*\}^\top \{(\mathbf{c}_k^m)^\ell - (\mathbf{c}_k^m)^*\} \right]}_{(\text{A})} = 0. \end{aligned}$$

Formula (A) turns out to be zero because of the first optimality condition of (S.2). Thus, we can prove

$$\lim_{\ell \rightarrow \infty} \left[V(\mathcal{A}^\ell) + \lambda \sum_{j,k} \|\boldsymbol{\beta}_{jk}^\ell\|_2 + \gamma \sum_{m,k} \|(\mathbf{c}_k^m)^\ell\|_1 \right] = V(\mathcal{A}^*) + \lambda \sum_{j,k} \|\boldsymbol{\beta}_{jk}^*\|_2 + \gamma \sum_{m,k} \|(\mathbf{c}_k^m)^*\|_1.$$

Next, we prove that $\lim_{\ell \rightarrow \infty} \|\boldsymbol{\theta}^\ell - \boldsymbol{\theta}^*\|_2 = 0$ holds whenever $\boldsymbol{\theta}^*$ is a unique solution. Since $\mathcal{L}(\boldsymbol{\theta})$ is a convex function, we can directly apply the proof of Ye and Xie (2011) by replacing $\Phi(\boldsymbol{\beta})$ in Ye and Xie (2011) with $\mathcal{L}(\boldsymbol{\theta})$. This completes the proof of Theorem 1. \square

S2 Additional figures in the Monte Carlo simulations

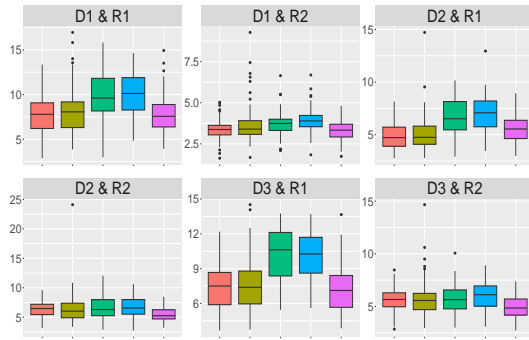
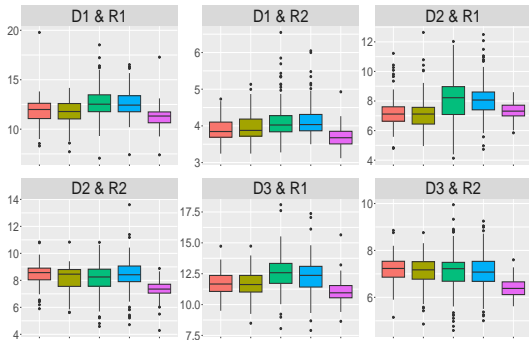
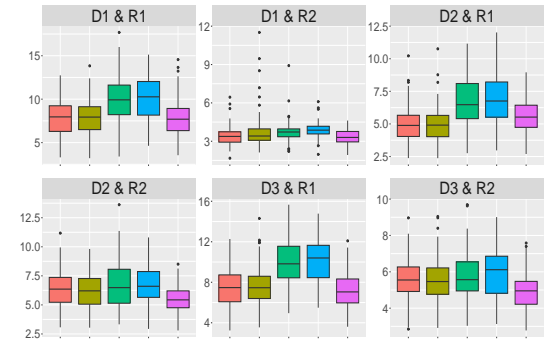
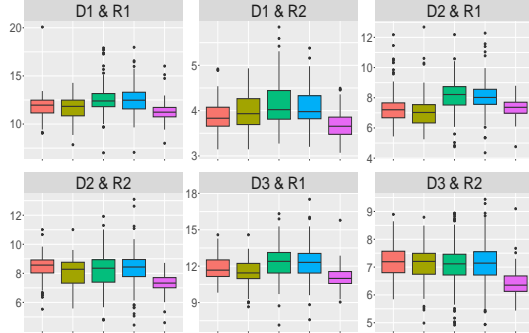
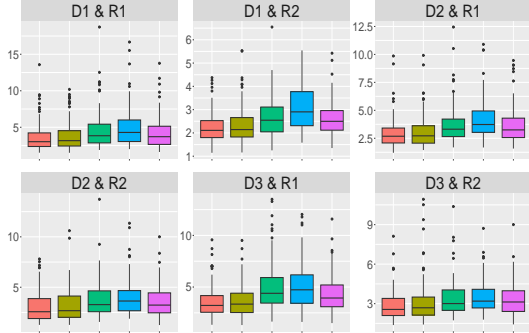
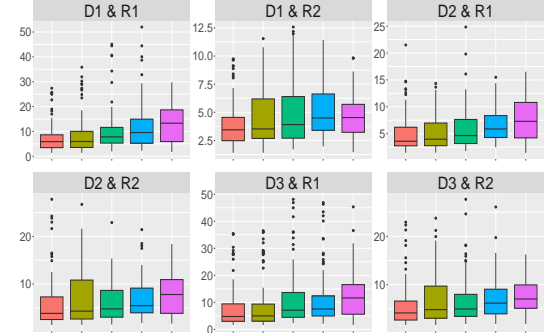
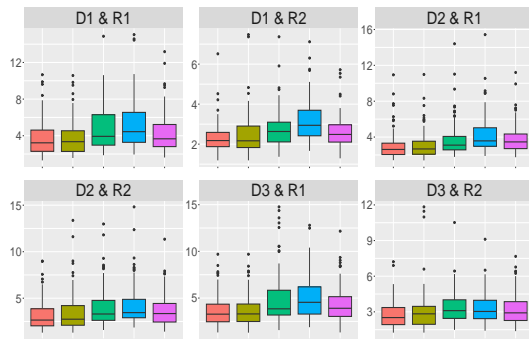
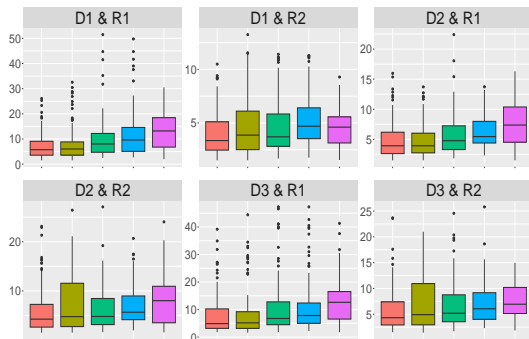
(a) $s = 5, \rho_x = 0.1, \rho_y = 0.1$ (b) $s = 50, \rho_x = 0.1, \rho_y = 0.1$ (c) $s = 5, \rho_x = 0.1, \rho_y = 0.9$ (d) $s = 50, \rho_x = 0.1, \rho_y = 0.9$ (e) $s = 5, \rho_x = 0.9, \rho_y = 0.1$ (f) $s = 50, \rho_x = 0.9, \rho_y = 0.1$ (g) $s = 5, \rho_x = 0.9, \rho_y = 0.9$ (h) $s = 50, \rho_x = 0.9, \rho_y = 0.9$

Figure S.1: Boxplots of MSE for $n = 15$ when the case $M = 3$. The red boxplot indicates MR, dark yellow UR, green lasso, blue mglasso, and magenta mlasso.

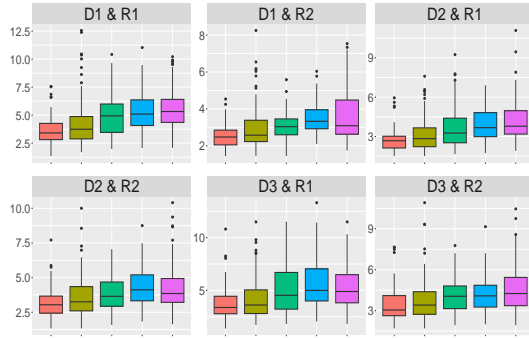
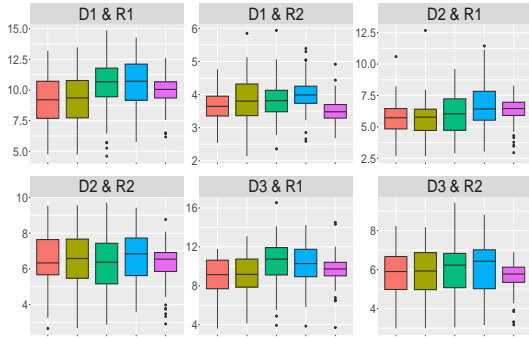
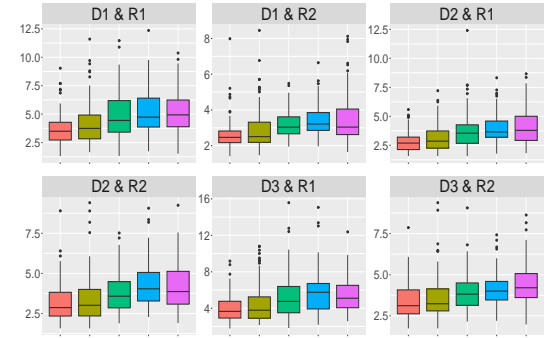
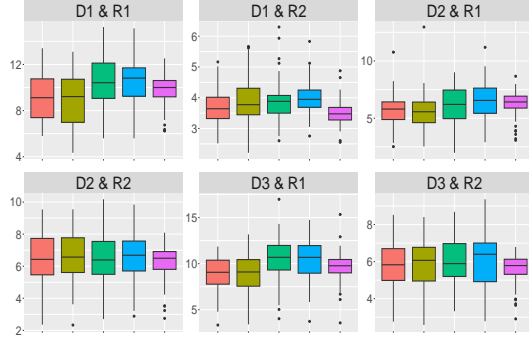
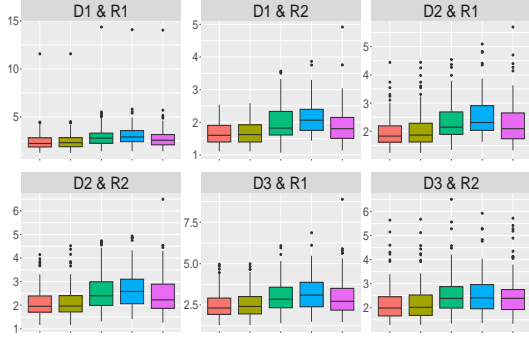
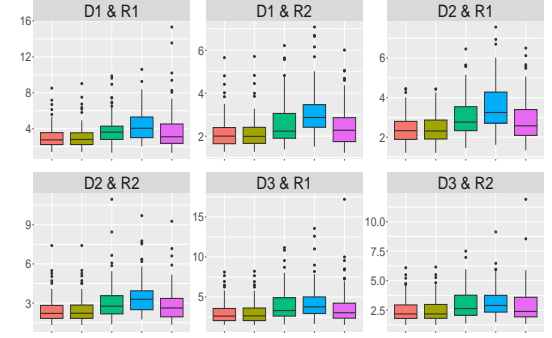
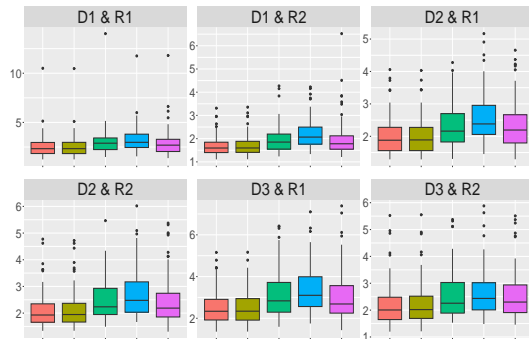
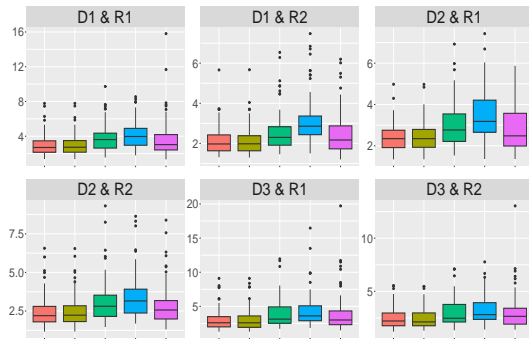
(a) $s = 5, \rho_x = 0.1, \rho_y = 0.1$ (b) $s = 50, \rho_x = 0.1, \rho_y = 0.1$ (c) $s = 5, \rho_x = 0.1, \rho_y = 0.9$ (d) $s = 50, \rho_x = 0.1, \rho_y = 0.9$ (e) $s = 5, \rho_x = 0.9, \rho_y = 0.1$ (f) $s = 50, \rho_x = 0.9, \rho_y = 0.1$ (g) $s = 5, \rho_x = 0.9, \rho_y = 0.9$ (h) $s = 50, \rho_x = 0.9, \rho_y = 0.9$

Figure S.2: Boxplots of MSE for $n = 25$ when the case $M = 3$. The red boxplot indicates MR, dark yellow UR, green lasso, blue mglasso, and magenta mlasso.

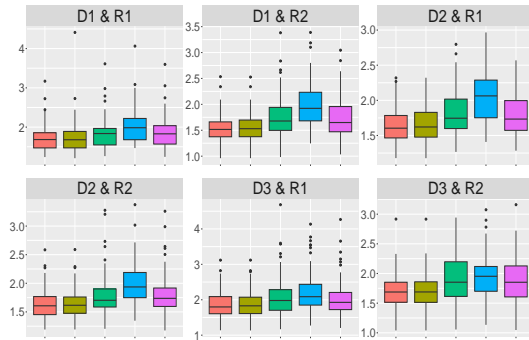
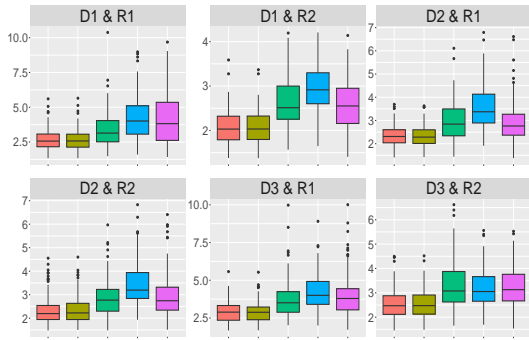
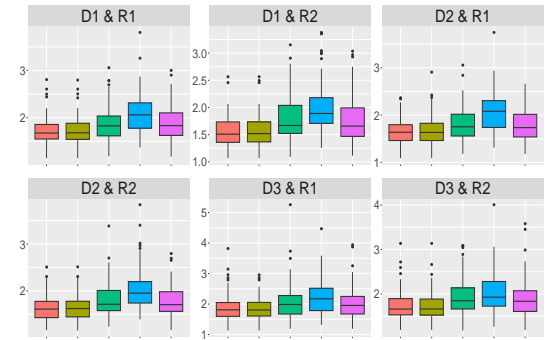
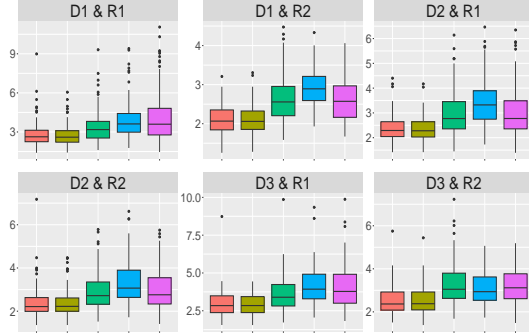
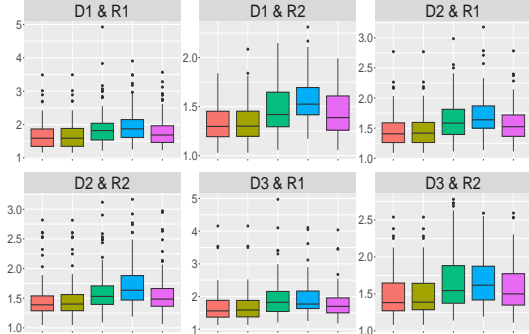
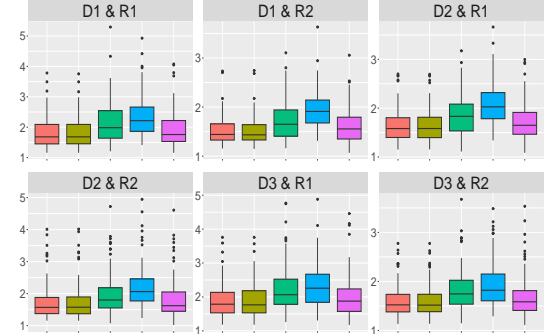
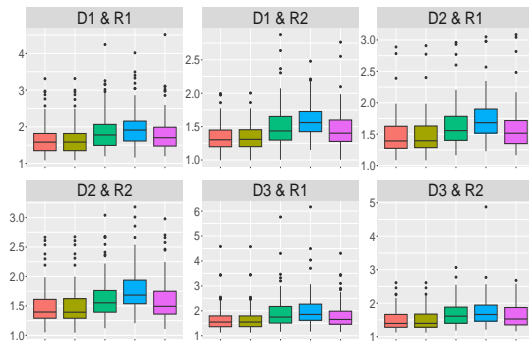
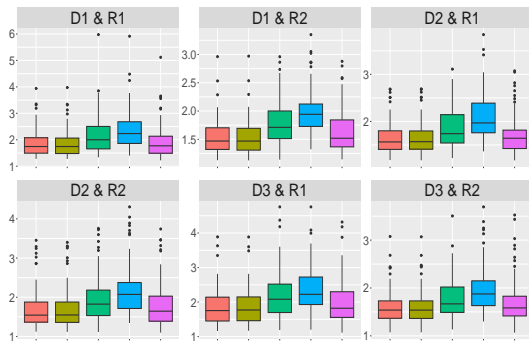
(a) $s = 5, \rho_x = 0.1, \rho_y = 0.1$ (b) $s = 50, \rho_x = 0.1, \rho_y = 0.1$ (c) $s = 5, \rho_x = 0.1, \rho_y = 0.9$ (d) $s = 50, \rho_x = 0.1, \rho_y = 0.9$ (e) $s = 5, \rho_x = 0.9, \rho_y = 0.1$ (f) $s = 50, \rho_x = 0.9, \rho_y = 0.1$ (g) $s = 5, \rho_x = 0.9, \rho_y = 0.9$ (h) $s = 50, \rho_x = 0.9, \rho_y = 0.9$

Figure S.3: Boxplots of MSE for $n = 50$ when the case $M = 3$. The red boxplot indicates MR, dark yellow UR, green lasso, blue mgllasso, and magenta mlasso.

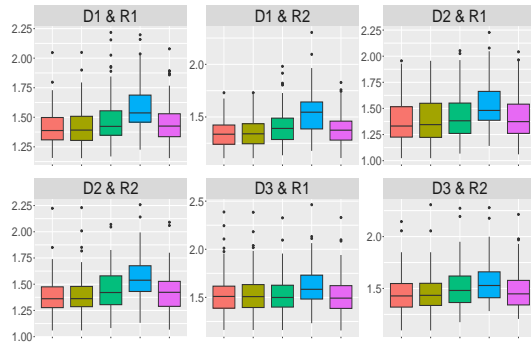
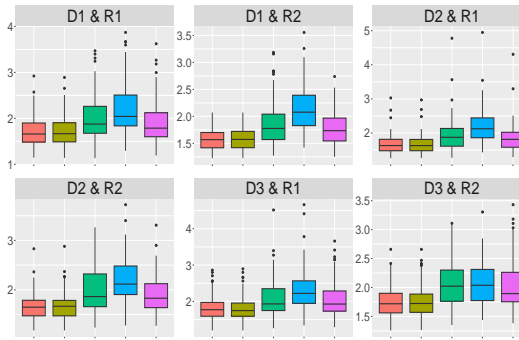
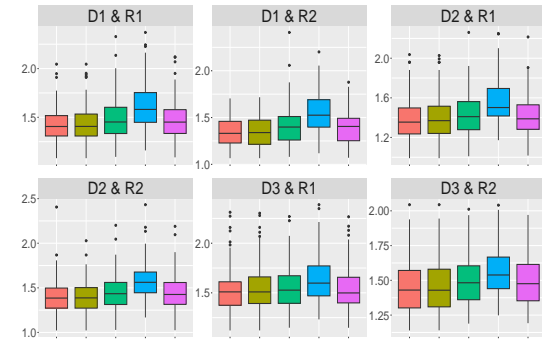
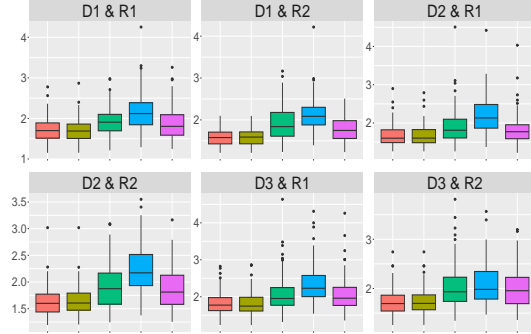
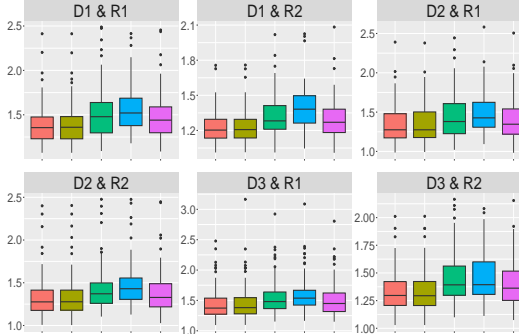
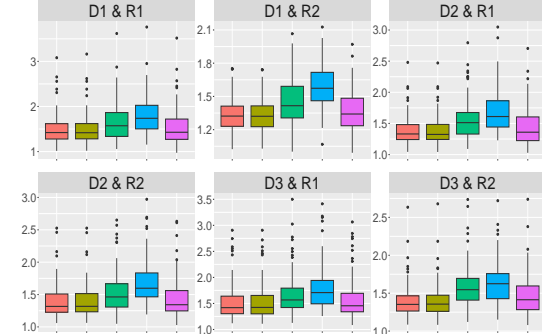
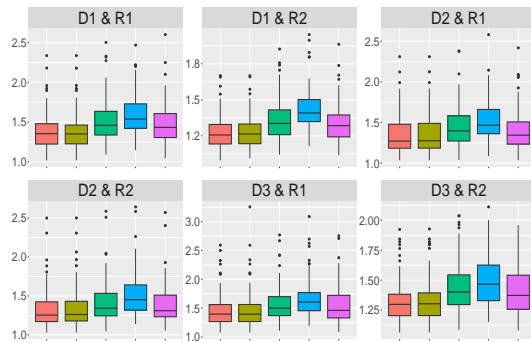
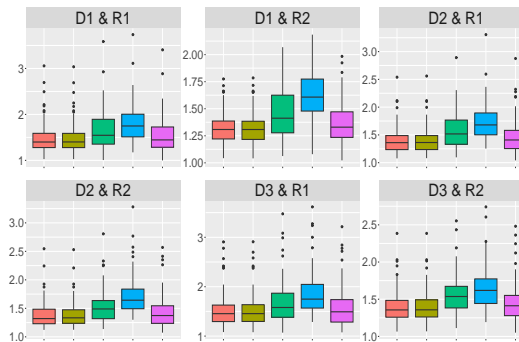
(a) $s = 5, \rho_x = 0.1, \rho_y = 0.1$ (b) $s = 50, \rho_x = 0.1, \rho_y = 0.1$ (c) $s = 5, \rho_x = 0.1, \rho_y = 0.9$ (d) $s = 50, \rho_x = 0.1, \rho_y = 0.9$ (e) $s = 5, \rho_x = 0.9, \rho_y = 0.1$ (f) $s = 50, \rho_x = 0.9, \rho_y = 0.1$ (g) $s = 5, \rho_x = 0.9, \rho_y = 0.9$ (h) $s = 50, \rho_x = 0.9, \rho_y = 0.9$

Figure S.4: Boxplots of MSE for $n = 75$ when the case $M = 3$. The red boxplot indicates MR, dark yellow UR, green lasso, blue mglasso, and magenta mlasso.

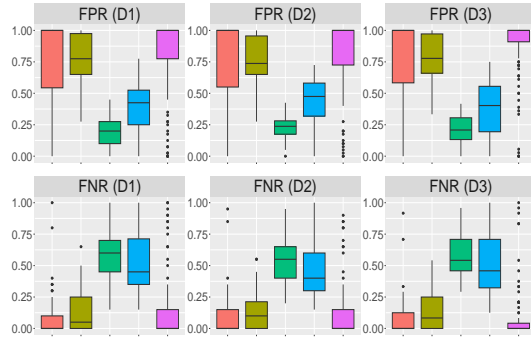
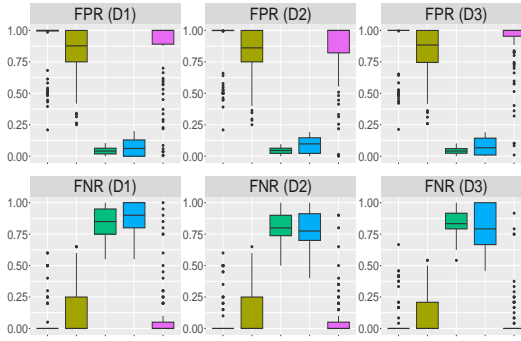
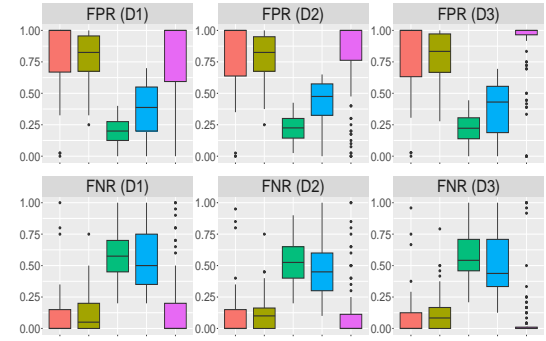
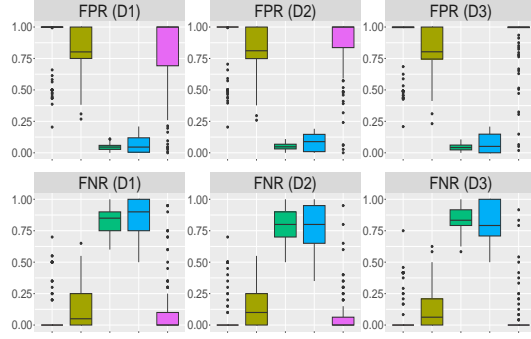
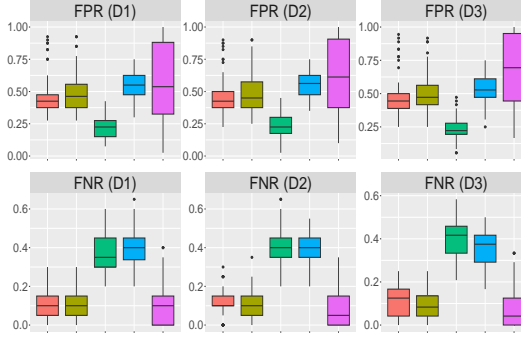
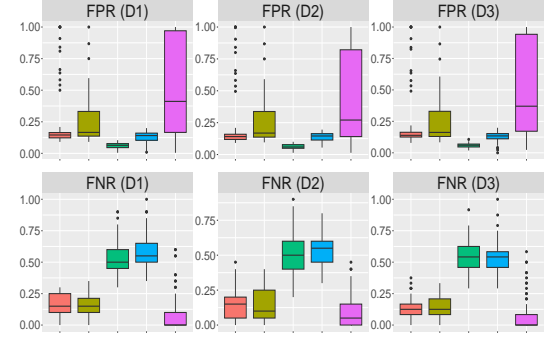
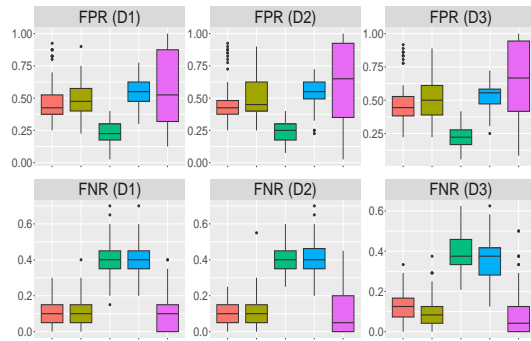
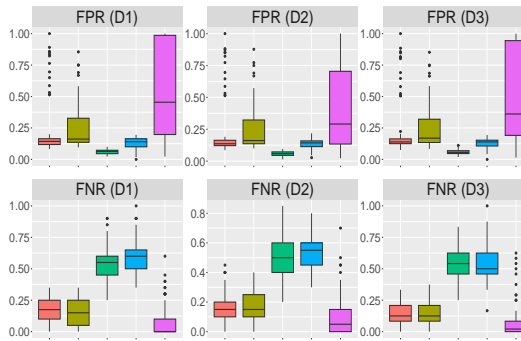
(a) $s = 5, \rho_x = 0.1, \rho_y = 0.1$ (b) $s = 50, \rho_x = 0.1, \rho_y = 0.1$ (c) $s = 5, \rho_x = 0.1, \rho_y = 0.9$ (d) $s = 50, \rho_x = 0.1, \rho_y = 0.9$ (e) $s = 5, \rho_x = 0.9, \rho_y = 0.1$ (f) $s = 50, \rho_x = 0.9, \rho_y = 0.1$ (g) $s = 5, \rho_x = 0.9, \rho_y = 0.9$ (h) $s = 50, \rho_x = 0.9, \rho_y = 0.9$

Figure S.5: Boxplots of FPR and FNR for $n = 15$ when the case $M = 3$. The red boxplot indicates MR, dark yellow UR, green lasso, blue mglasso, and magenta mllasso.

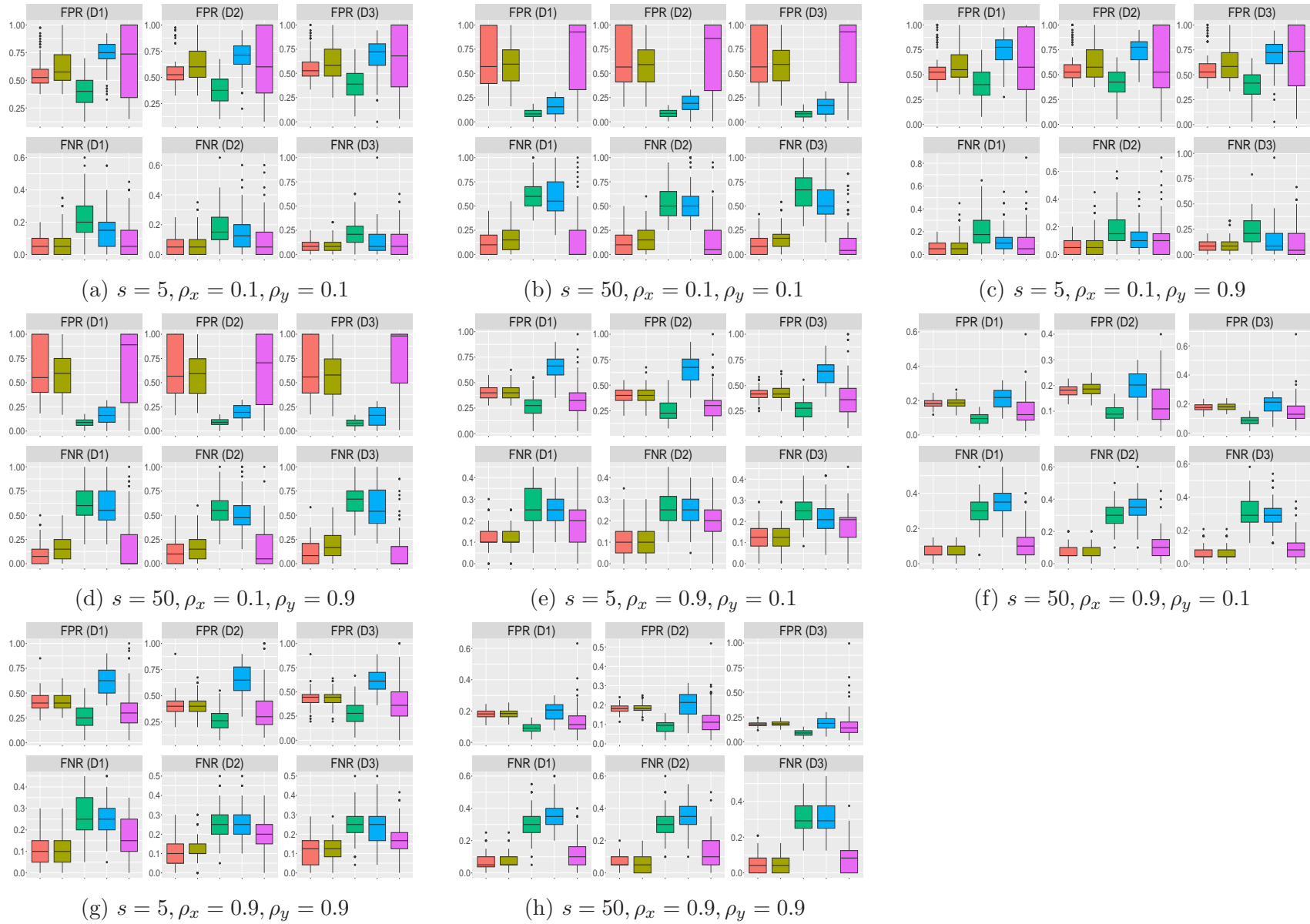


Figure S.6: Boxplots of FPR and FNR for $n = 25$ when the case $M = 3$. The red boxplot indicates MR, dark yellow UR, green lasso, blue mglasso, and magenta mlasso.



Figure S.7: Boxplots of FPR and FNR for $n = 50$ when the case $M = 3$. The red boxplot indicates MR, dark yellow UR, green lasso, blue mglasso, and magenta mlasso.



Figure S.8: Boxplots of FPR and FNR for $n = 75$ when the case $M = 3$. The red boxplot indicates MR, dark yellow UR, green lasso, blue mglasso, and magenta mlasso.